Title

Dynamic integration of conceptual information during learning

Journal

PLOS ONE, 13(11)

ISSN

1932-6203

Authors

Inhoff, Marika C

Libby, Laura A

Noguchi, Takao

et al.

Publication Date

2018

DOI

10.1371/journal.pone.0207357

Peer reviewed

PLOS ONE

RESEARCH ARTICLE

Dynamic integration of conceptual information during learning

Marika C. Inhoff[1], Laura A. Libby[2], Takao Noguchi[3], Bradley C. Love[3,4], Charan Ranganath[1,2]*

1 Department of Psychology, University of California at Davis, Davis, CA, United States of America, **2** Center for Neuroscience, University of California at Davis, Davis, CA, United States of America, **3** Department of Experimental Psychology, University College London, London, United Kingdom, **4** Alan Turing Institute, Kings Cross, London, United Kingdom

* cranganath@ucdavis.edu

Citation: Inhoff MC, Libby LA, Noguchi T, Love BC, Ranganath C (2018) Dynamic integration of conceptual information during learning. PLoS ONE 13(11): e0207357. https://doi.org/10.1371/journal.pone.0207357

Editor: Emmanuel Andreas Stamatakis, University of Cambridge, UNITED KINGDOM

Received: March 12, 2018

Accepted: October 30, 2018

Published: November 14, 2018

Data Availability Statement: Data are available from the Open Science Framework (https://osf.io/zdmw8/).

Funding: This work was supported by the National Science Foundation Graduate Research Fellowship to MCI (#1148897) https://www.nsfgrfp.org/; the Leverhulme Trust (RPG-2014-075) and Wellcome Trust Senior Investigator Award WT106931MA to BCL; A National Institute of Mental Health grant R01MH068721, a Guggenheim Fellowship, the Vannevar Bush Fellowship (Office of Naval Research Grant N00014-15-1-0033) and a Multi-

Abstract

The development and application of concepts is a critical component of cognition. Although concepts can be formed on the basis of simple perceptual or semantic features, conceptual representations can also capitalize on similarities across feature relationships. By representing these types of higher-order relationships, concepts can simplify the learning problem and facilitate decisions. Despite this, little is known about the neural mechanisms that support the construction and deployment of these kinds of higher-order concepts during learning. To address this question, we combined a carefully designed associative learning task with computational model-based functional magnetic resonance imaging (fMRI). Participants were scanned as they learned and made decisions about sixteen pairs of cues and associated outcomes. Associations were structured such that individual cues shared feature relationships, operationalized as shared patterns of cue pair-outcome associations. In order to capture the large number of possible conceptual representational structures that participants might employ and to evaluate how conceptual representations are used during learning, we leveraged a well-specified Bayesian computational model of category learning [1]. Behavioral and model-based results revealed that participants who displayed a tendency to link experiences in memory benefitted from faster learning rates, suggesting that the use of the conceptual structure in the task facilitated decisions about cue pair-outcome associations. Model-based fMRI analyses revealed that trial-by-trial integration of cue information into higher-order conceptual representations was supported by an anterior temporal (AT) network of regions previously implicated in representing complex conjunctions of features and meaning-based information.

Introduction

One of the core functions of memory is the ability to use prior experience to optimize and facilitate decisions. A central challenge to this adaptive behavior, however, is the dense and continuous nature of experience. One approach to reducing this complexity is to make use of conceptual structure in the environment. Concepts can be formed on the basis of simple

University Research Initiative Grant (Office of Naval Research Grant N00014-17-1-2961) from the Office of Naval Research to CR. Any opinions, findings, and conclusions or recommendations expressed in this material are those of the authors and do not necessarily reflect the views of the Office of Naval Research or the U.S. Department of Defense.

Competing interests: The authors have declared that no competing interests exist.

features (e.g. 'has feathers' to categorize animals as birds), however concepts are also thought to reflect broader forms of featural overlap, which can include the similarity of the relationships between features [1,2]. For example, concepts reflecting two different types of coins can be formed based on shared information about their value inside a fairground and at a convenience store. Tokens and medallions can be used to pay for items at a fairground but are worthless at a convenience store, whereas quarters and dimes possess the opposite set of value relationships. Concepts like "carnival currency" or "world currency" can support decision-making and efficient learning about individual coins by allowing for inferences across different coins that share feature relationships [3].

Although recent neuroimaging investigations have begun to elucidate the brain regions that support conceptual or category membership on the basis of simple features [4–11], little is known about the neural mechanisms involved in the development and use of conceptual representations based on shared relationships across features. To address this question we combined a carefully designed associative learning task with computational model-based fMRI. Participants were scanned as they learned about sixteen pairs of novel cue objects and deterministically associated outcomes. Each trial began with the sequential presentation of a pair of object cues and a prompt to predict the associated outcome followed by response feedback. Critically, relationships between pairs of cues and outcomes formed a network of overlapping associations, where groups of cues shared identical cue pair and outcome associations, or identical feature relationships. These shared feature relationships could serve to simplify the learning problem from sixteen individual cue pair-outcome associations into four higher-order concepts, reflecting groups of cue-pair outcome associations containing individual cues with shared feature relationships (Fig 1). Importantly, this reduction of the learning problem was adaptive, and could allow for the acceleration of learning and facilitation of decisions in the task.

In order to elucidate the processes involved in building concepts based on shared feature relationships and to understand how they are represented in the brain, we turned to computational model-based fMRI. Specifically, we fit a well-specified Bayesian computational model of category learning [1] to trial-by-trial learning behavior, allowing for the generation of process-based estimates of dissociable aspects of the conceptual structure used by each participant during learning. We focused on two model estimates associated with the separate cue and outcome phases of each trial: "Cue-based integration" and "Feedback-based updating". Cue-based integration reflects the likelihood that a participant will use the shared feature relationships to assign cue pairs to an existing conceptual cluster rather than generating a novel conceptual cluster for the cue pair. "Feedback-based updating," reflects changes to the broader conceptual cluster space, or the full set of existing conceptual clusters, as participants receive and learn from response feedback.

Recent models suggest that two different cortical networks [12–14] might play key roles in supporting Cue-based integration and Feedback-based updating. Specifically, a large number of investigations have linked regions in an "Anterior Temporal" (AT) network, including the perirhinal cortex (PRc) and orbitofrontal cortex (OFC), to the meaning of objects and integration of complex conjunctions of object features [4,15–23]. These findings led us to hypothesize that activity in the AT network might track Cue-based integration. On the other hand, regions in a "Posterior Medial" (PM) network, including the parahippocampal cortex (PHc) [24–32], retrosplenial cortex (RSC) [33–36], and angular gyrus [37,38], have been shown to support memory for contextual information. Given that shared feature relationships in this task rely on the local context of each trial, or the trial-wise associations between cue pair and outcome, we might expect the PM network to index Cue-based integration. Alternatively, we might expect the PM network to be preferentially involved in tracking Feedback-based updating, or trial-by-trial

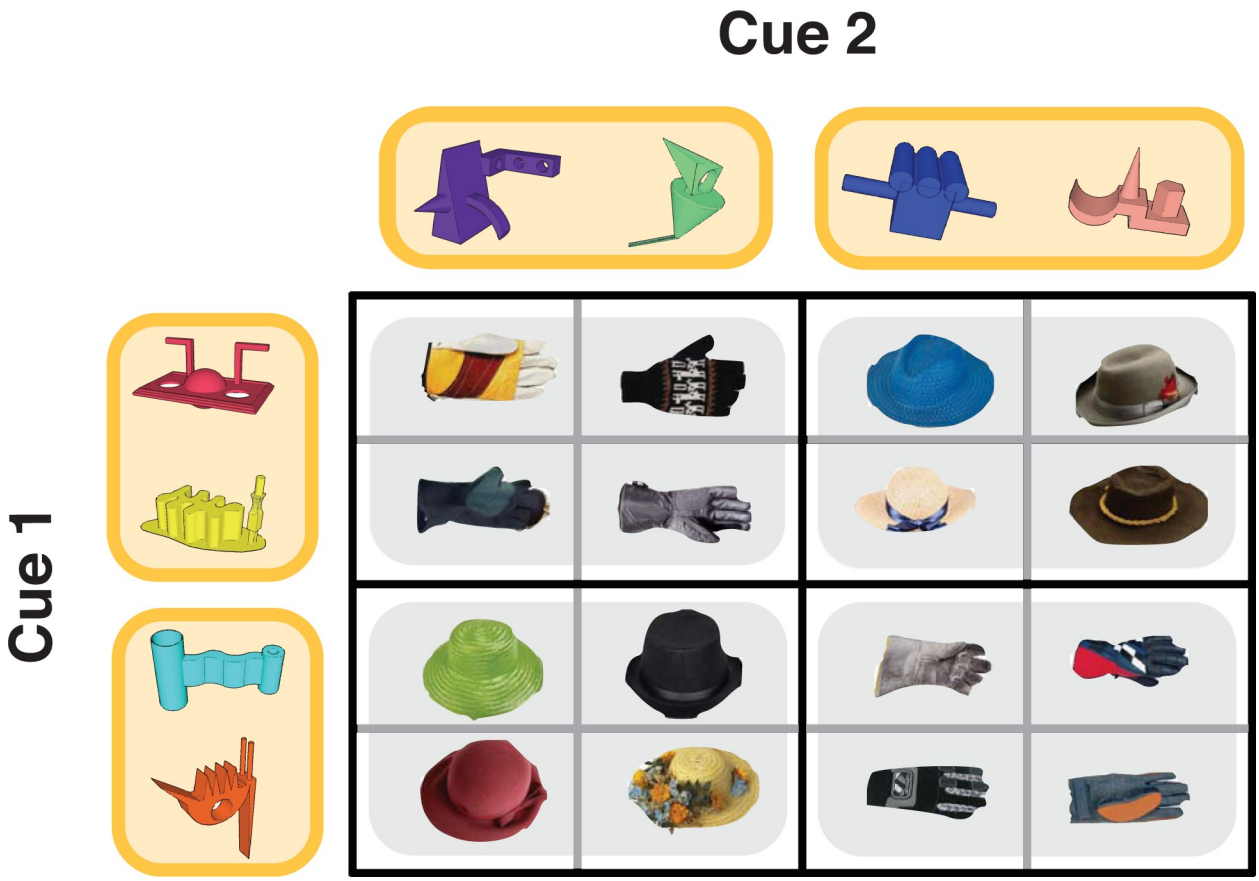

Fig 1. Task structure. Sixteen unique trial sequences of Cue 1, Cue 2, and outcome objects were constructed for each participant. In this example task structure, Cue 1 objects are presented along the y-axis, Cue 2 are objects presented along the x-axis, and associated Outcomes are presented in the center of the grid. For example, when the magenta Cue 1 is paired with the green Cue 2, the associated outcome is a glove. Individual cue objects each have a 50% chance of association with a Hat or Glove category outcome, requiring participants to use information about the Cue 1 –Cue 2 pair to make correct decisions. Cue 1—Cue 2—Outcome associations were fully crossed to create four pairs of cue objects that share feature relationships (highlighted in yellow). For example, both the magenta and yellow Cue 1 objects are associated with a glove category outcome when paired with the purple or green Cue 2 object and a hat category outcome when paired with the blue or tan Cue 2 object. This design gives rise to four groupings of Cue 1—Cue 2—Outcome associations where the corresponding cue objects create triplets with maximal conceptual overlap (highlighted in grey).

https://doi.org/10.1371/journal.pone.0207357.g001

changes to the conceptual cluster space following response feedback, given proposals that that the PM network represents the full set of relevant relationships in the environment [13].

Materials and methods

Subjects

This research was approved by the Institutional Review Board at the University of California at Davis (IRB #637028). Written consent was obtained from all participants. Thirty-one (20 female) participants from the University of California at Davis community enrolled in the experiment. Two participants were excluded due to falling asleep inside the scanner, one participant was excluded due to excessive motion, and three participants were excluded due to issues with scanner protocol specifications. Of the remaining 25 participants (17 female), all had normal or corrected-to-normal vision, were native English speakers, and were 18 to 31 years of age. Participants were paid $50 for their participation, and received

additional compensation for the proportion of responses made above chance level on their best learning run (maximum additional payment of $5).

Stimuli

To control for any use of semantic or perceptual information in learning cue pair-outcome associations, eight novel object stimuli were manually generated using Google SketchUp software (http://www.sketchup.com). Cue objects were designed to be visually distinctive in shape and color. Eight unique hat and eight unique glove outcome objects were selected from a stimulus database of objects [39].

Design

Participants were scanned while completing six runs of a learning task. Each trial of the learning task began with the sequential presentation of two cue objects (Cue 1 and Cue 2) and an associated outcome. Importantly, each individual Cue object was associated with a 50% probability of predicting a hat or glove category outcome, requiring participants to integrate the combination of Cue 1 and Cue 2 to correctly predict the associated outcome category (Fig 1). Cue pair-outcome associations were generated by randomly assigning four of the eight novel objects to Cue 1, and the remaining four novel objects to Cue 2. To create a higher-order conceptual structure, cue pair-outcome associations were crossed to create pairs of individual Cue objects that shared feature relationships, or that shared patterns of cue pair-outcome associations (Fig 1, cues that share feature relationships highlighted in yellow). We reasoned that cue-pair outcome associations comprised of Cue 1 and Cue 2 objects with shared feature relationships would have maximal conceptual overlap (Fig 1, highlighted in grey).

Experimental procedure

The experiment was comprised of four parts: unscanned target detection practice, one scanned pre-learning target detection run, six runs of scanned learning, one scanned post-learning target detection run, and a final unscanned memory test. Only the data from the scanned learning period were included for analysis.

During the six scanned learning runs, participants were presented with trials consisting of sequentially presented Cue1 –Cue 2 –outcome associations (Fig 2). Each trial began with the presentation of a Cue 1 object in the center of the screen for 2 seconds, followed by a blank screen for 500 ms. After the presentation of Cue 1, a Cue 2 object was presented for 2 seconds with the words 'hat' and 'glove' printed underneath, referring to the possible category-level outcomes. Participants were asked to use their pointer or middle finger to predict the category-level outcome associated with the current Cue 1 –Cue 2 pair. Response buttons were counterbalanced across participants. Following the 2 second Cue 2 period, a 500 ms blank screen was presented, followed by outcome information and response feedback. Specifically, participants were presented with a unique hat or glove associated with the Cue 1 –Cue 2 pair, as well as feedback on the category-level decision made during the Cue 2 period. Each Cue 1 –Cue 2 –Outcome association was presented three times per run, and trial order was pseudo-randomly determined by drawing without replacement from the sixteen Cue 1 –Cue 2 –Outcome associations three times, with no back-to-back repetitions of individual associations. This resulted in three iterations through the full set of sixteen cue pair-outcome associations, for a total of forty-eight trials per learning run. A variable ITI with a static fixation cross followed each trial, and lasted between 1 and 4 seconds, with a mean of 3 seconds. Each run lasted approximately 8 minutes and 17 seconds with approximately 7 minutes and 48 seconds of this period associated with task performance. Each run began with 7 TRs (approximately 8.5

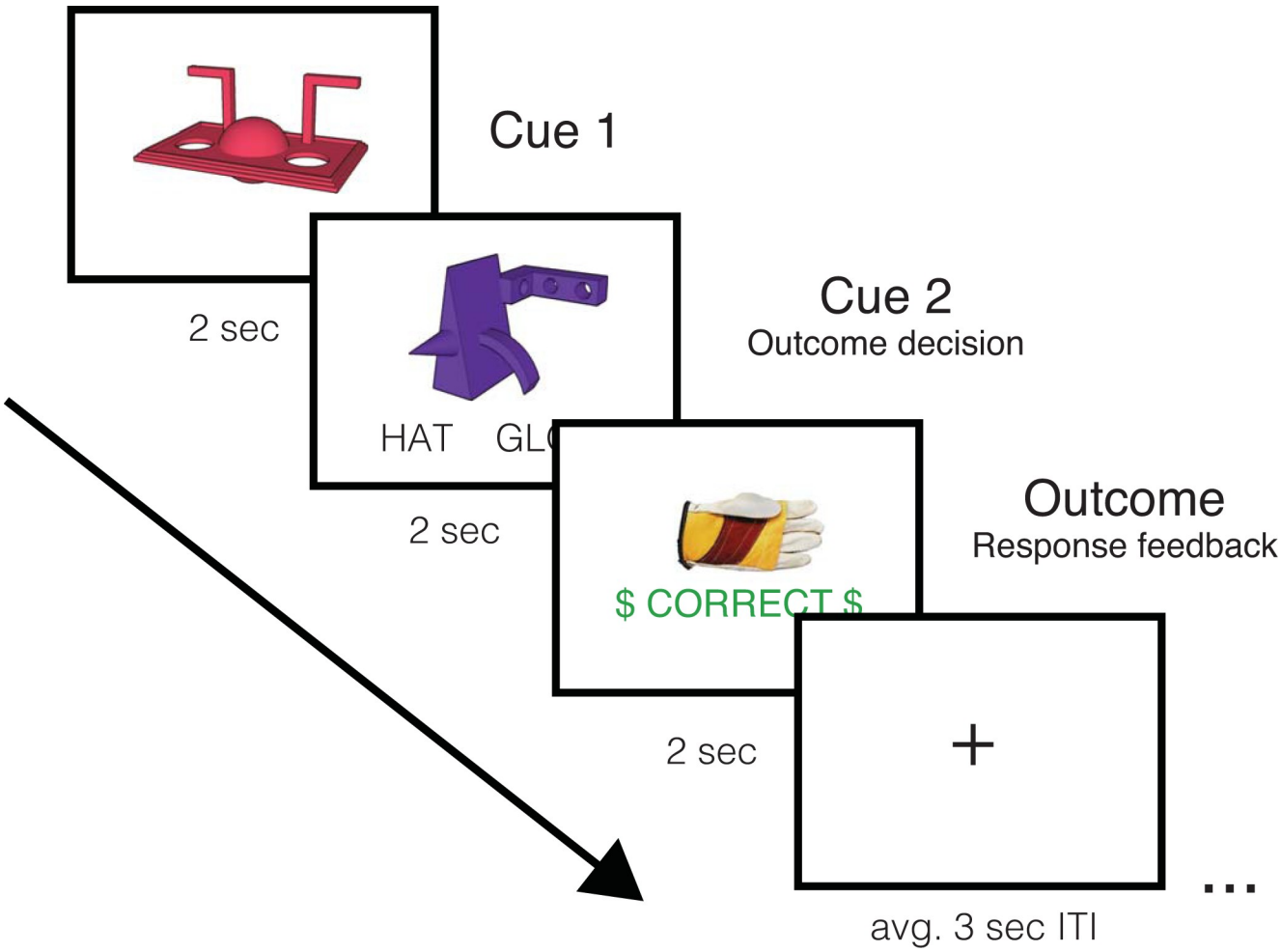

Fig 2. Trial sequence during scanned learning. Participants were presented with Cue 1, Cue 2 and Outcome feedback information sequentially.

https://doi.org/10.1371/journal.pone.0207357.g002

seconds) of a white fixation cross presented on a black screen to allow for fMRI signal stabilization and ended with 7 TRs (approximately 8.5 seconds) of a white fixation cross presented on a black screen to capture the duration of the hemodynamic response. In addition to trial-by-trial feedback, participants were presented with information about the proportion of trials they had answered correctly at the end of each learning run.

Model-based analyses

Although the learning task was comprised of sixteen individual cue pair-outcome associations, the contingencies between cue objects and outcomes were designed such that participants could facilitate learning by integrating across cue pairs that contained Cue items with similar cue pair-outcome relationships (Fig 1). However, we expected large individual differences in the degree to which a participant could learn and use the conceptual structure of the task to guide learning. To accommodate this variance and to gain leverage on the processes that supported learning, we used the Rational Model of Categorization (RMC) to model behavioral data from the learning task [1]. We chose to apply the RMC based on previous theory [40] linking clustering mechanisms to key regions of interest and related model-based fMRI studies [5,41].

The RMC assumes that categories are learned by clustering similar stimuli together. Suppose a learner has observed $n-1$ stimuli $\{x_1, x_2, \ldots, x_{n-1}\}$ with corresponding category labels $\{y_1, y_2, \ldots, y_{n-1}\}$. Each stimulus is fit into a cluster $\{z_1, z_2, \ldots, z_{n-1}\}$. In the context of present study, x_i is a pair of cues presented at the ith trial, and y_i is a corresponding category outcome. An exact object which followed a cue pair (e.g., green hat and black glove) is denoted as $\tilde{y}_i$. If the cue pair x_i was fit into the jth cluster, z_i equals to j.

Now, let us suppose $w(0 < w < n)$ clusters have been formed after $n-1$ trials. Then, the probability that the cue pair at the nth trial is judged to be from category h follows Bayesian inference:

$$\begin{aligned} p(y_n = h \mid x_n) &= \sum_{k \in \{1,2,\ldots,w\}} p(z_n = k \mid x_n) p(y_n = h \mid z_n = k) \\ &= \sum_{k \in \{1,2,\ldots,w\}} \frac{p(z_n = k) p(x_n \mid z_n = k)}{\sum_{s \in \{1,2,\ldots,w\}} p(z_n = s) p(x_n \mid z_n = s)} p(y_n = h \mid z_n = k) \end{aligned} \quad (1)$$

The three terms in Eq 1 is described below in turn.

First, the probability that the nth cue pair fits into the kth cluster is given by

$$p(z_n = k) = \begin{cases} \dfrac{c m_k}{(1-c) + c(n-1)} & \text{if } m_k > 0 \\ \dfrac{1-c}{(1-c) + c(n-1)} & \text{if } m_k = 0 \end{cases}$$

where c is a parameter called the coupling probability, and m_k is the number of cue pairs already assigned to the kth cluster.

The coupling probability is a single value for each participant that reflects the sensitivity in generating new clusters or to linking information to existing clusters in memory. A smaller coupling probability, for example, indicates that a new cluster is more likely to be created to accommodate the nth cue pair. Conversely, a larger coupling probability indicates that information is likely to be linked with an existing cluster. Thus, individual differences in learning can be captured by allowing the coupling probability parameter to vary across participants.

We assume that cues are independent of each other [1,42]:

$$p(x_n \mid z_n = k) = \prod_{d \in \{1,2\}} p(x_{n,d} \mid z_n = k)$$

Here, $x_{n,d}$ denotes the dth cue in the cue pair at the nth trial. This term is calculated with

$$p(x_{n,d} = v \mid z_n = k) = \frac{B_{v,d} + \beta_c}{m_k + 4\beta_c},$$

where β_c is the sensitivity parameter for a cue, and $B_{v,d}$ the number of cue pairs in the kth cluster whose dth cue is v.

Similarly, the probability that the nth cue pair is from category h given a cluster is given by

$$p(y_n = h \mid z_n = k) = \frac{B_h + \beta_l}{m_k + 2\beta_l},$$

where β_l is the sensitivity parameter for a category, and B_h is the number of cue pairs in the kth cluster whose category is h. Unlike the coupling probability, the sensitivity parameter was not allowed to vary between participants.

After observing outcomes associated with each cue pair, a learner assigns a cue pair to a cluster. This cluster assignment also follows Bayesian inference, where the probability that the *n*th cue pair fits into the *k*th cluster is given by

$$p(z_n = k \mid x_n, y_n, \tilde{y_n}) \propto p(z_n = k)p(x_n \mid z_n = k)p(y_n \mid z_n = k)p(\tilde{y_n} \mid z_n = k).$$

The last term is given by

$$p(\tilde{y_n} = g \mid z_n = k) = \frac{B_g + \beta_l}{m_k + 2\beta_l},$$

where B_g is the number of cue pairs in the *k*th cluster which is associated with object *g* (e.g., green hat).

This learning by clustering is probabilistic, and the same parameter values can result in different cluster formulations. To account for this stochasticity, we simulated the model 2,000 times with one particle when evaluating a set of parameters [42]. This stochastic learning allows for a characterization of dissociable processes involved in using the conceptual cluster space.

To obtain trial-by-trial measures, we estimated the maximum a posteriori of parameter values (the coupling probability and the sensitivity parameters) using the Bayesian optimization framework. The prior distribution for the coupling probability was the uniform distribution between 0 and 1, and the prior distribution for the sensitivity parameters was the uniform distribution between 0.01 and 10. The estimated parameter values are: the coupling probability ranges from 0.0002 to 0.0373 with a mean of 0.0088, and the sensitivity parameters are 0.01 for both cue and outcome category. With these parameter values, we took mean average of trial-by-trial measures from the 2,000 simulations.

In order to elucidate the involvement of PM and AT networks, we focused on two model-derived measures reflecting the trial-by-trial development and use of concepts during different phases of each trial: "Cue-based integration," and "Feedback-based updating." Cue-based integration is a measure assessing the likelihood that participants will assign or integrate a pair of cues to an existing conceptual cluster rather than generating a novel conceptual cluster for the cue pair. Using the above notation, the Cue-based integration estimate is given by $\frac{(1-c)}{(1-c)+c(n-1)}$. Feedback-based updating, on the other hand, assesses how much the conceptual cluster space changes following feedback. Thus, Feedback-based updating indicates the extent to which one learns and modifies their knowledge based on the outcome of each individual trial. Feedback-based updating is quantified as the Kullback-Leibler divergence between the probability distributions over the clusters before and after the feedback: $p(z_i|x_i)$ and $p(z_i \mid x_i, y_i, \tilde{y}_i)$.

FMRI methods

MRI scans were acquired at the UC Davis Imaging Research Center using a 3T Siemens Skyra equipped with a 32-channel head coil. Participants were supplied with earplugs to attenuate scanner noise, and head padding was used to reduce motion. Stimuli were presented visually on a screen at the back of the scanner, and viewed through a mirror attached to the head coil. T1-weighted structural images were acquired with a magnetization-prepared rapid acquisition gradient echo (MPRAGE) pulse sequence (1 mm^3 voxels; matrix size = 256 x 256; 208 slices) and images sensitive to BOLD contrast were acquired using a whole-brain multiband gradient echo planar imaging sequence (3 mm^3 voxels; TR = 1220ms; TE = 24ms; FA = 67˚; multiband acceleration factor = 2; 38 interleaved slices; FOV = 192 mm; matrix size = 64 x 64).

Preprocessing and analysis of functional MRI data was conducted with FSL FEAT (FMRIB Software Library, https://fsl.fmrib.ox.ac.uk/fsl/fslwiki). The first 7 volumes of each functional

run were discarded to allow for signal normalization. Preprocessing began with motion correction, which was applied using rigid body registration to the central volume using MCFLIRT [43]. Following this step, non-brain removal was conducted using FSL's brain extraction tool BET [44]. Next, a Gaussian spatial smoothing was applied using a kernel of 6.0 mm full width at half maximum. After this step, grand-mean intensity normalization of the entire 4D dataset by a single multiplicative factor was conducted. Finally, high-pass temporal filtering was also applied (Gaussian-weighted least-squares straight line fitting, with sigma 45.0s). Estimation of transformation matrices used to register functional data to the high resolution structural image (df = 6) and standard MNI152 template (df = 12) was also carried out using FLIRT as part of a standard preprocessing pipeline [43,45]. Time-series statistical analysis was carried out using FILM with local autocorrelation correction [46].

Regions of interest

As noted earlier, our hypotheses centered on the roles of the AT and PM networks in using the higher-order conceptual structure of the task to guide learning. To address this question, we used thirty-six regions of interest (ROIs) within the PM and AT networks (18 AT ROIs, 18 PM ROIs). PMAT ROIs were defined as 6 mm spheres centered on coordinates identified in an independent dataset on the basis of a comparison of PHc and PRc resting-state functional connectivity (RSFC) [47]. Spheres were non-overlapping and spatially separated by a distance of at least 12 mm. PMAT network assignment of each sphere was determined on the basis of resting state networks identified in a separate independent dataset [48]. To determine network assignment in this independent dataset, Ritchey et al. applied a community detection algorithm to RSFC time courses extracted from the spheres identified based on functional connectivity [47], allowing for an identification of spheres that showed greater within vs. between network connectivity [48]. All analyses were conducted on PMAT ROIs that were in standard MNI space.

FMRI statistical analysis

We conducted three fMRI analyses to assess the involvement of the PM and AT networks in indexing dissociable aspects of learning in a task with a higher-order conceptual structure. To assess network involvement in the conceptual integration of cue pairs with shared feature relationships ("Cue-based integration") and incremental updating of the conceptual cluster space ("Feedback-based updating"), we conducted a computational model-based fMRI analysis. In order to rule out whether the results of the model-based analyses could be attributed to task performance alone, we also conducted a separate accuracy-based univariate analysis assessing PM and AT network activation during the cue pair and outcome periods of correct relative to incorrect trials. Finally, in order to provide evidence supporting dissociable PM and AT networks in the current task, we conducted an activation profile similarity analysis using estimates from both the model- and accuracy-based analyses.

Computational model-based fMRI analysis. The RMC was individually fit to each participant's learning data to generate trial-by-trial estimates of Cue-based integration and Feedback-based updating (see section on *Model-based analyses*). Task activation was assessed using a parametric univariate analysis implemented in FSL. Individual modulated and unmodulated regressors were constructed for each iteration through the full set of Cue 1 –Cue 2 –Outcome associations (three iterations per run). Model-derived estimates were modeled on an iteration-by-iteration basis to avoid confounding model-based learning measures with effects related to time and other random variance. To estimate neural activation associated with the conceptual integration of cue pairs with shared feature relationships, three model-derived Cue-based integration parametric regressors (one for each iteration) were included in the first-level GLM.

Parametric regressors for Cue-based integration were modeled at the onset of Cue 1 with a duration of 4.5 seconds to include the full Cue 1 and Cue 2 presentation period. To estimate neural activation associated with the updating of the conceptual cluster space in response to feedback information ("Feedback-based updating"), three model-based parametric regressors reflecting Feedback-based updating were also included. Each Feedback-based updating parametric regressor was modeled at the onset of the Feedback period with a duration of 2 seconds. Cue and Feedback-based parametric regressors were mean-corrected separately on an iteration-by-iteration basis. To model the mean activation associated with the Cue period, three 4.5 second unmodulated boxcars (one regressor for each iteration) were modeled at the onset of Cue 1 with a duration of 4.5 seconds. Mean activation associated with the Feedback period was modeled similarly, with three separate 2 second unmodulated boxcars (one regressor for each iteration) beginning at the onset of Feedback. The first iteration of the first learning run was modeled as a 7 second unmodulated nuisance regressor to allow for stabilization of model estimates following one complete iteration through the full set of cue-pair outcome associations. Regressors were convolved with a double-gamma hemodynamic response function prior to model estimation.

In order to assess the parametric effects of Cue-based integration and Feedback-based updating in each run, first level contrasts for Cue-based integration and Feedback-based updating were computed separately. Contrasts included regressors from all iterations. To average contrast estimates over all six learning runs, a second-level fixed effects model was carried out by forcing the random effects variance to zero in FLAME (FMRIB's Local Analysis of Mixed Effects) [49–51]. Participant-level statistical contrast maps for Cue-based integration and Feedback-based updating were registered to standard MNI template space for subsequent analysis using the transformation matrix estimated during preprocessing of each participant's data.

To characterize the roles of the PM and AT networks in Cue-based integration and Feedback-based updating, mean parameter estimates were extracted for each ROI from each contrast and averaged within network, yielding four estimates per participant (AT network–Cue-based integration, PM network–Cue-based integration, AT network–Feedback-based updating, PM network–Feedback-based updating). Contrast estimates were submitted to a repeated-measures ANOVA assessing the effects of Network (PM, AT) and Trial period (cue, feedback), and followed up with planned two-tailed paired comparisons.

Accuracy-based fMRI analysis. To rule out whether parametric activation associated with Cue-based integration and Feedback-based updating was merely a reflection of task accuracy, we conducted a separate accuracy-based analysis to assess cue and feedback activation during trials with correct relative to incorrect category outcome decisions. In order to ensure sufficient trial numbers to estimate contrasts for correct and incorrect trials, functional data from runs one through three were concatenated into an "Early learning" period, and functional data from runs three through six were concatenated to create a "Late learning" period. First-level modeling of each learning period included four regressors of interest for the cue and outcome periods of trials associated with correct and incorrect category outcome decisions. Additionally, two unconvolved nuisance regressors were included to model the effect of run. To assess cue and feedback-based activation for correct > incorrect trials across early and late learning, a second-level fixed-effects model was carried out by forcing the random effects variance to zero in FLAME [49–51]. Participant-level statistical contrast maps for Cue: correct > incorrect and Feedback: correct > incorrect were transformed to standard MNI template space for subsequent analysis using the transformation matrix estimated during preprocessing of each participant's data. Subject-level contrast estimates were extracted for each ROI from each contrast and averaged, yielding four estimates per network per participant (AT network–Cue: correct > incorrect; PM network–Cue: correct > incorrect; AT network–

Feedback: correct > incorrect; PM network–Feedback: correct > incorrect). Contrast estimates were submitted to a repeated-measures ANOVA assessing the effects of Network (PM, AT) and Trial period (cue, feedback), and followed up with two-tailed t-tests to assess planned paired comparisons.

Activation profile similarity analysis. In order to validate our analyses on data from the AT and PM networks, we tested the appropriateness of grouping individual ROIs according to this network framework. Following Ritchey et al. [48] we ran an "activation profile similarity analysis," to test whether regions in the same putative network showed more similar profiles of activation across the different experimental conditions than did regions in different networks. Mean subject-level contrast estimates from each condition of interest (Cue-based integration; Feedback-based updating; Cue: correct > incorrect; Feedback: correct > incorrect) were z-transformed and extracted from each ROI. This procedure yielded an activation matrix with a separate four-element activation vector for each ROI. To measure the similarity of activation profiles across all pairs of ROIs, the activation matrix was correlated using Pearson's *r* and sorted by network affiliation. In order to assess functional homogeneity within network, the resulting activation similarity correlation matrix was compared to a model matrix, where pairs of ROIs within the same network were represented with a value of 1 (perfect correlation) and ROI pairs in different networks were represented with a value of 0 (no correlation). Both the activation similarity correlation matrix and model matrix were vectorized and compared with Kendall's tau-b, a non-parametric measure of statistical dependence. Additionally, activation similarity correlation values were averaged across regions within the PM and AT networks (within-network) and compared to the average across regions in the PM and AT networks (between-network). Correlation values were Fisher z-transformed prior to comparison via a two-tailed paired t-test.

Results

Behavioral results and computational model fits

Behavioral performance indicated that participants were, on average, able to learn associations between pairs of cues and outcomes across six learning runs (Fig 3). When submitting average performance across runs to a repeated-measures ANOVA, there was a significant main effect of Run [$F_{5,120} = 39.5$, $p < .000001$], indicating that outcome decisions improved significantly across the six task runs. Consistent with this idea, outcome decisions were not significantly different from chance (50%) until the fourth ($p < 0.05$, binomial test), fifth ($p < .0001$, binomial test) and sixth ($p < .0001$, binomial test) task runs. Additionally, outcome decision reaction times were found to decrease significantly across runs [$F_{5,120} = 2.82$, $p < .05$]. Despite a group-level improvement in performance across learning runs, there was a large amount of variability in individual participant ability to learn Cue 1 –Cue 2 –Outcome associations (Fig 3). As such, the standard deviation of the group accuracy score (percent correct) increased from 0.06 in the first run to .18 on the final learning run.

Next, we assessed whether individual participant behavioral estimates from the RMC were able to approximate subject performance during the learning task (Fig 4). On average, the R^2 across all participants was .46 with a standard error of +/- 0.057, suggesting that the RMC provides a good fit to the observed behavioral data despite the large amount of variability observed across participants.

Linking of experiences in memory is associated with facilitated learning

Although the task consisted of sixteen individual cue-pair outcome associations, capitalizing on shared feature relationships could reduce the learning problem and facilitate correct outcome decisions. To assess evidence in support of this idea, we turned to the coupling

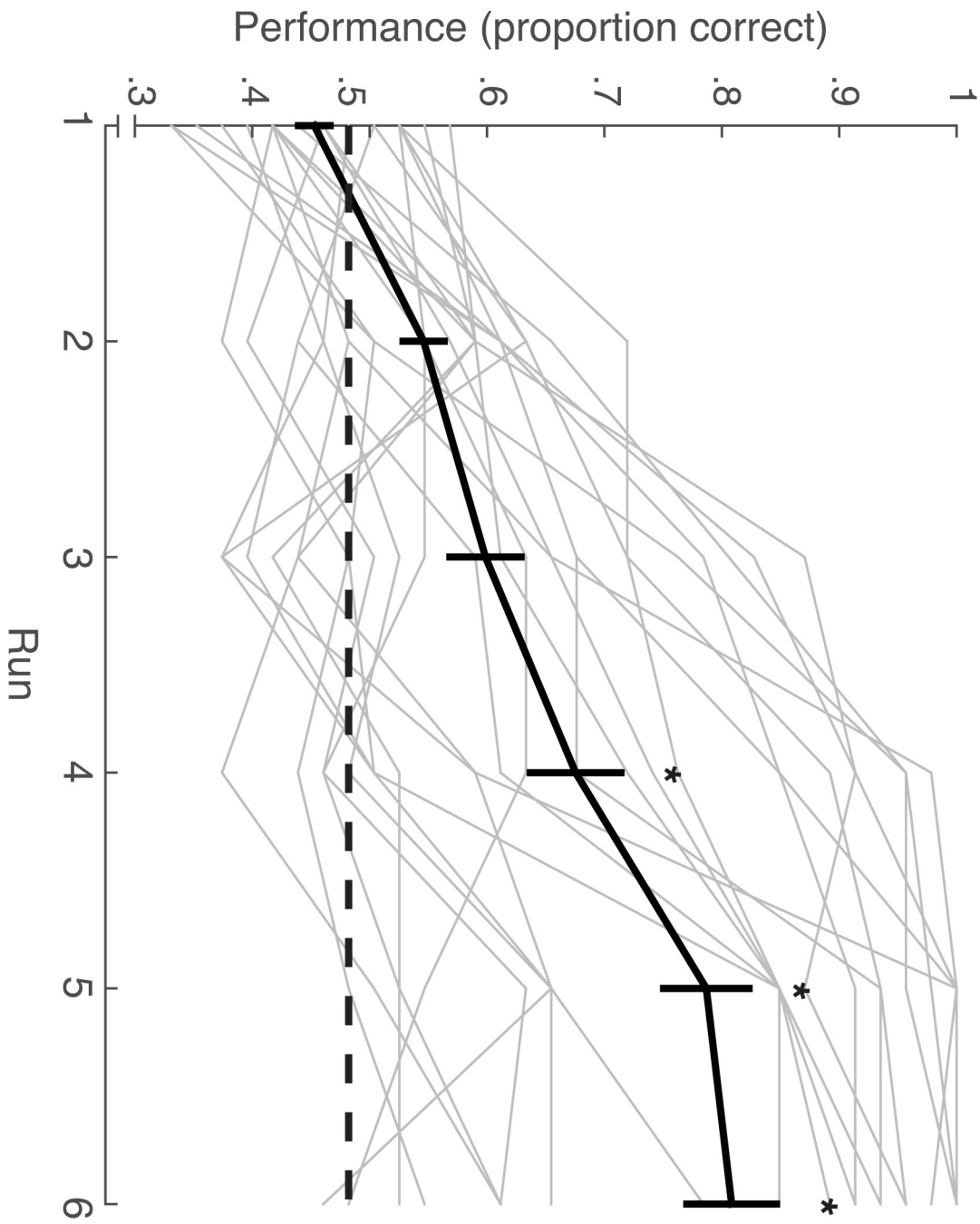

Fig 3. Learning performance. On average, participants gradually learned to choose outcomes correctly across six runs of scanned learning, however there was a large amount of variability in individual participant performance. Chance performance (50%) is plotted by a dashed line. Mean subject performance plotted in black. Individual subject learning curves plotted in grey. Error bars reflect standard error of the mean. * $p < .05$, binomial test.

https://doi.org/10.1371/journal.pone.0207357.g003

probability, or a single model-derived value that describes each participant's tendency to link cue pair-outcome associations (see section on *Model-based analysis*). We observed a significant positive correlation between the coupling probability and the slope of each participant's learning curve. Specifically, larger coupling probabilities were associated with faster learning rates in the task (Fig 5, [$r(24) = .7507$, $p < .0001$]).

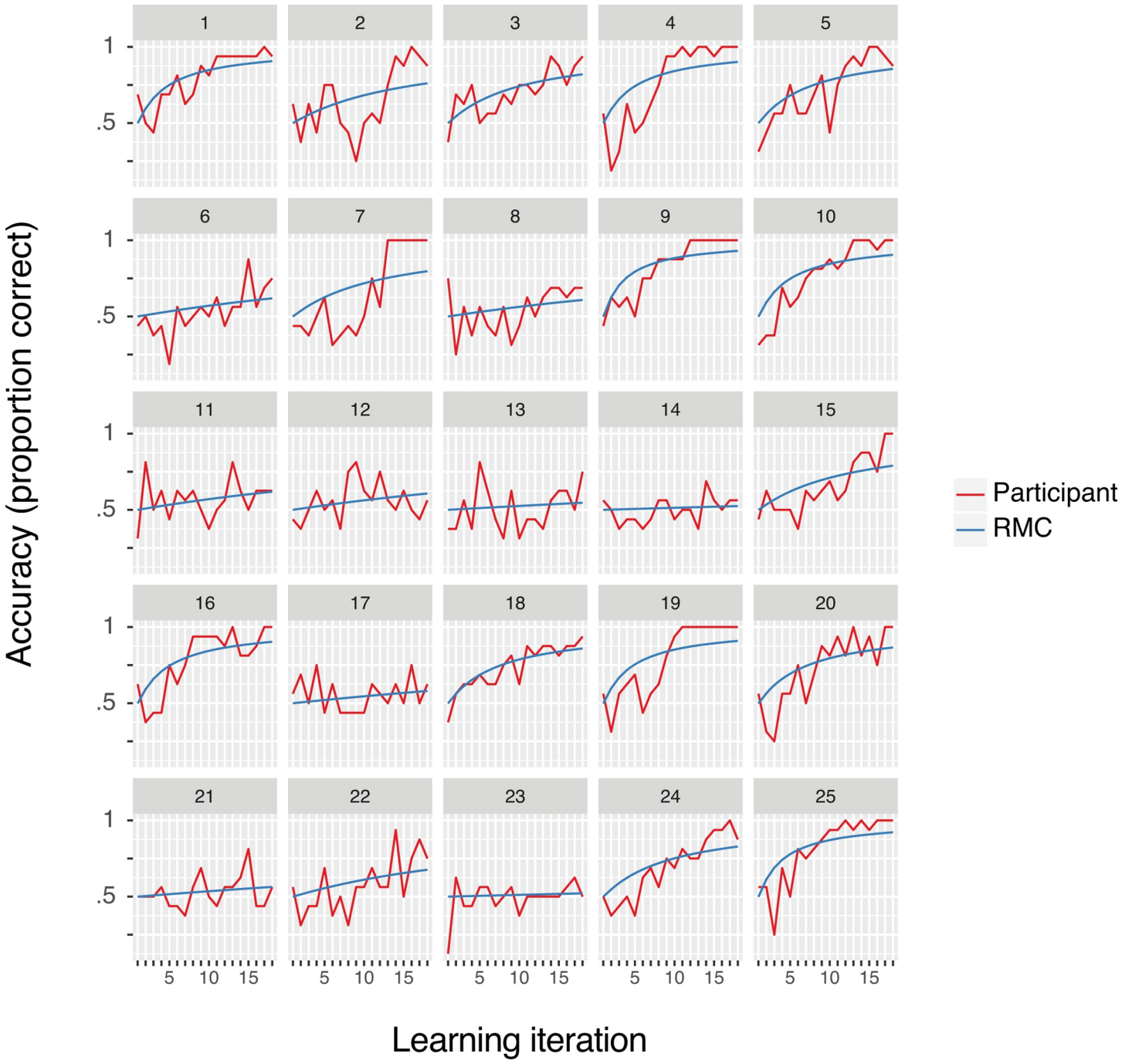

Fig 4. Individual participant behavioral model fits. Iteration through each full set of 16 cue pair-outcome associations is plotted on the x-axis (iterations 1 through 3 correspond to Run 1, iterations 4 through 6 correspond to Run 2, and so on). Accuracy (proportion correct) is plotted along the y-axis. Each participant's learning performance is plotted in red with the corresponding RMC learning curve in blue. On average, the RMC provides a good fit to the observed behavioral data.

https://doi.org/10.1371/journal.pone.0207357.g004

Evidence for dissociable PM and AT networks

As noted earlier, prior evidence is consistent with the idea that regions in the AT or PM networks (or both) could contribute to dissociable aspects of learning conceptual information in this task. Prior work suggests that there is substantial similarity in the extent to which regions

within the same network are recruited during different task conditions [48]. To conceptually replicate these results and to verify the appropriateness of grouping ROIs according to the PMAT framework [13], we conducted an activation profile similarity analysis [48] in which we quantified the similarity of task-based activation profiles across regions within and across each network (Fig 6). If individual ROIs are operating in concert with other within-network regions and processing similar types of information in the learning task, we should see similar activation values across regions that belong to the same network. Additionally, this relationship should be true for activation values derived from all available contrasts.

Activation profile similarity scores are computed by correlating univariate activation vectors across all pairs of ROIs within and across networks. A pair of ROIs will display high correlation, or high activation profile similarity, if both regions exhibit a comparable pattern of relative activation or deactivation across the four contrasts derived from the computational model- and accuracy-based analyses (Model–Cue-based integration; Model–Feedback-based updating; Accuracy–Cue: correct > incorrect; Accuracy–Feedback: correct > incorrect). To assess whether regions within each network display similar activation profiles, correlation values were sorted by network affiliation, vectorized, and compared with an idealized model matrix, where correlations between regions within the same network were represented as 1 (perfect correlation) and correlations for ROI pairs in different networks were represented as 0 (no correlation). The Kendall's tau-b correlation between activation profile similarity values and the model matrix was statistically significant (Kendall's tau-b = .323, $p < .0001$), suggesting that activation profile similarity was higher across pairs of ROIs within the same network relative to ROI pairs across networks. A complimentary analysis directly comparing average within- relative to between-network correlations was consistent with these results, demonstrating significantly higher correlation values across pairs of ROIs within the same network relative to across networks [$t(24) = 8.11$, $p < .0001$]. Indeed, nearly every participant demonstrated higher within- relative to between-network activation profile similarity values, providing further evidence that regions in the PM and AT networks are engaged in separable processes as participants completed the task. We also conducted an additional analysis to determine the appropriateness of PMAT network organization in six participants who did not demonstrate behavioral evidence for learning cue-pair outcome associations (behavioral performance not significantly different from chance in the final two task runs). This analysis also revealed significantly greater within vs. between network activation profile similarity (see S1 Fig). Having established the validity of the distinction between the AT and PM networks, our next analyses focused on characterizing how these networks contributed to the development and use of conceptual information by relating them to two key indices from the computational model–Cue-based integration and Feedback-based updating.

Differential PM and AT network involvement in supporting Cue-based integration and Feedback-based updating

As noted in the introduction, there is good reason to think that the AT or PM networks, or both, would contribute to concept acquisition in this task. Based on previous work implicating the AT network in supporting information about the meaning of objects and complex conjunctions of features, we hypothesized that regions in this network should collectively track conceptual knowledge reflecting shared feature relationships. Alternatively, because shared feature relationships are built on the local context of each trial, one might expect regions in the PM network to preferentially represent Cue-based integration. A third possibility is that the AT and PM networks might play complementary roles in Cue-based integration. Building on recent proposals that the PM network supports representations of relevant relationships in the environment, we also hypothesized that this network would track trial-by-trial updates to the conceptual cluster space.

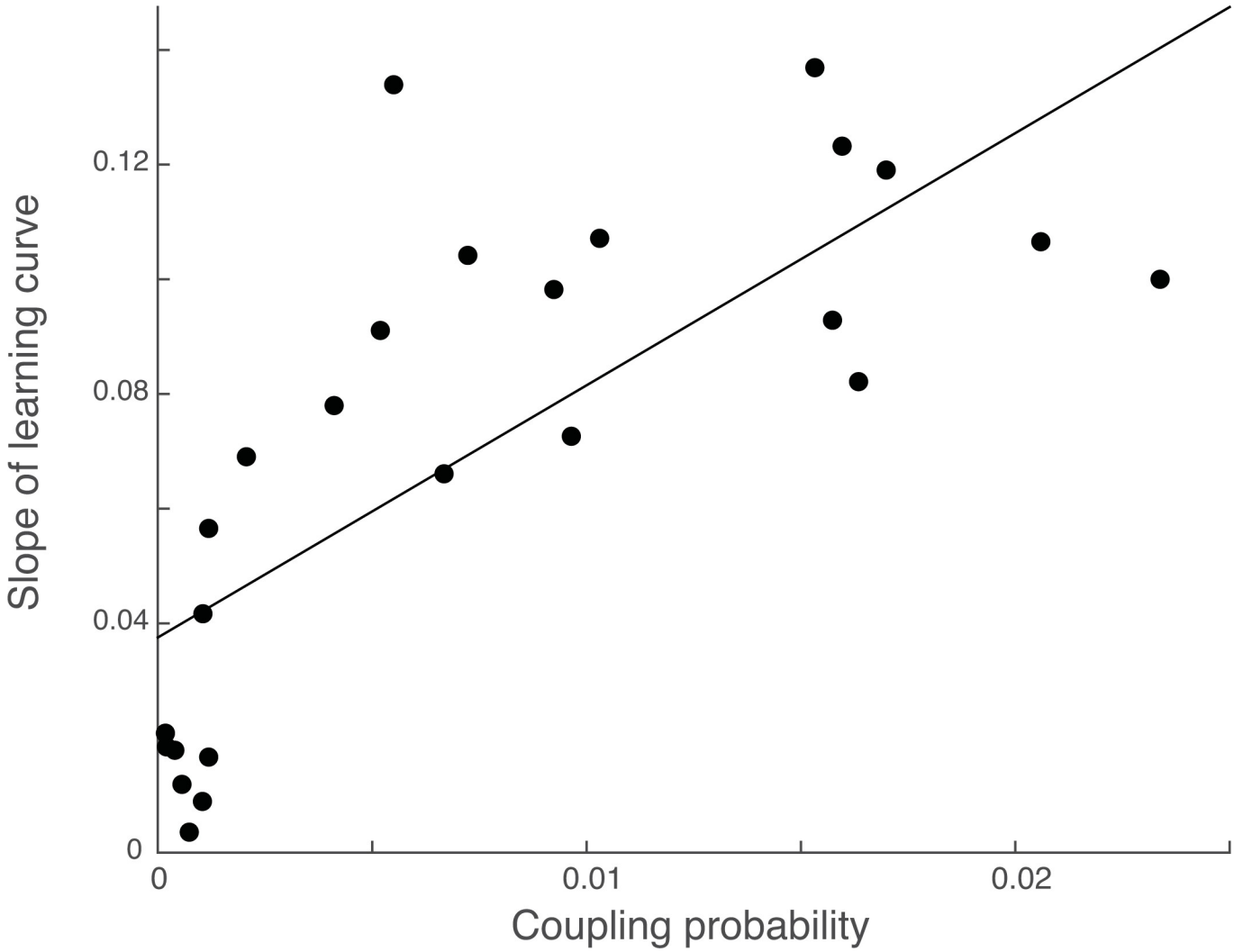

Fig 5. Larger coupling probabilities are associated with faster learning rates. Individual subject coupling probabilities, or a model-derived metric where higher values reflect a stronger tendency to link information in memory, is positively associated with the rate of learning.

https://doi.org/10.1371/journal.pone.0207357.g005

To test these hypotheses, parameter estimates indexing activation related to Cue-based integration and Feedback-based updating were submitted to a repeated measures ANOVA with factors for Network (PM, AT) and Trial period (cue, outcome). Results revealed a significant main effect of Network ($F_{1,24} = 9.89$, $p < .01$) and a significant Trial period by Network interaction ($F_{1,24} = 7.34$, $p < .012$) (Fig 7, left panel). No main effect of Trial period was observed ($F_{1,24} = 0.009$, $p = .92$). Follow-up paired comparisons revealed that Cue-based integration estimates were significantly lower in the AT network relative to the PM network [$t(24) = 3.22$, $p < .01$]. Additionally, one sample t-tests revealed that Cue-based integration parameter estimates were significantly different from zero in the AT network [$t(24) = -2.9$, $p < .01$] but were not significantly different from zero in the PM network [$t(24) = 1.36$, $p = 0.18$] (Fig 7A). Results were qualitatively similar but did not reach significance in analyses conducted on six participants who did not demonstrate evidence of learning cue-pair outcome associations (see S2 Fig, left panel). These results suggest that activity in the AT network reflected the integration of cue pair information into existing concepts, consistent with the use of the higher-order conceptual

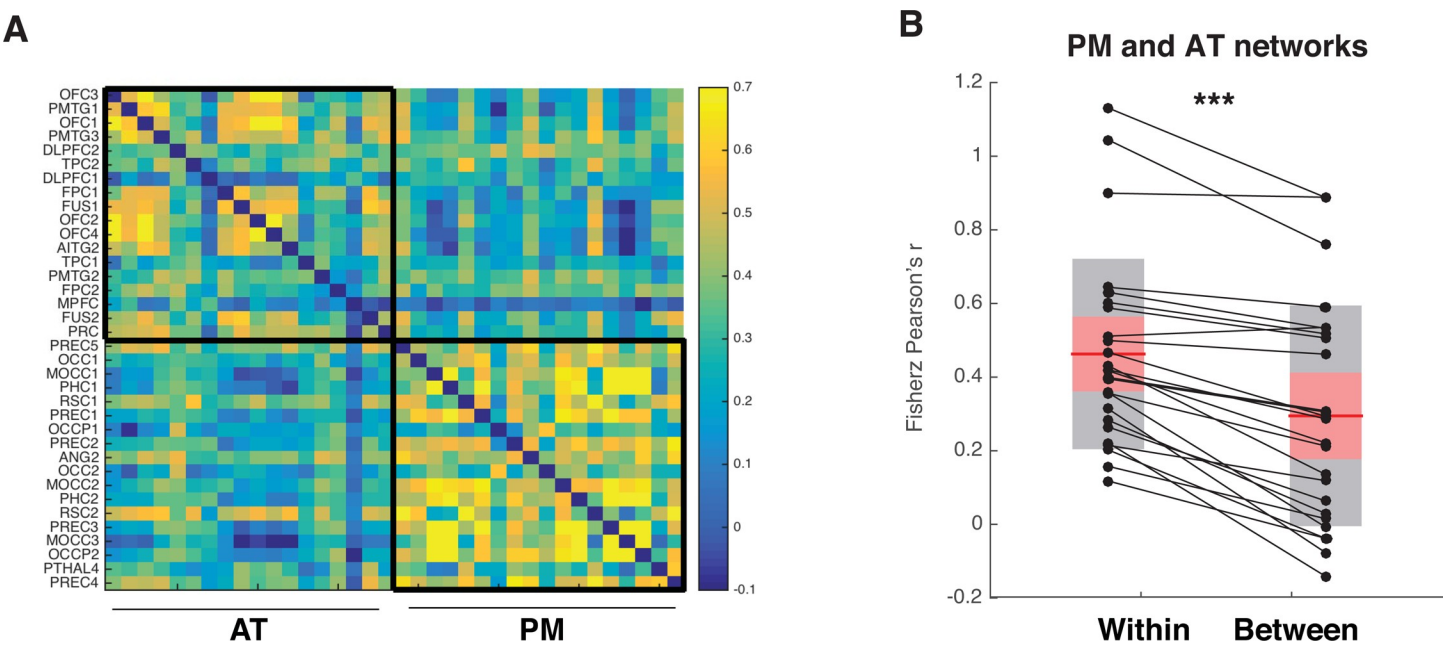

Fig 6. Activation profile similarity analysis. Regions within the PM and AT networks show high within but not between network activation profile similarity. (A) Activation profile similarity values were assessed by correlating mean z-transformed contrast values from each ROI extracted from each of the four contrasts of interest (Model–Cue-based prediction, Model–Feedback-based updating, Accuracy–Cue: Correct > Incorrect, Accuracy–Outcome: Correct > Incorrect). Higher correlation values indicate that a pair of ROIs displayed a more similar pattern of activation across contrasts. (B) Activation profile similarity correlations were significantly higher between ROIs that were from within the same network relative to across different networks. Grey-shaded box denotes standard deviation. Red shaded box denotes 95% confidence interval. Individual participant activation profile similarity values plotted in black. *** $p < .0001$.

https://doi.org/10.1371/journal.pone.0207357.g006

structure of the task. The PM network, on the other hand, did not display evidence for involvement in Cue-based integration.

There were also important differences in individual ROI responses to Cue-based integration and Feedback-based updating (see Fig 8). Within the AT network, ROIs in the posterior middle temporal gyrus (PMTG1, t(24) = -3.43, p = 0.002), anterior inferior temporal gyri (AITG2: t(24) = -2.38, p = 0.0254), and temporopolar cortex (TPC2: t(24) = -2.12, p = 0045) displayed significant evidence of integrating cue pairs into an existing conceptual cluster. In the PM network, precuneus (PREC5: t(24) = -2.64, p = 0.014) and retrosplenial cortex (RSC2: t (24) = -2.43, p = 0.023) also displayed significant evidence for cue-based integration, whereas occipital regions significantly tracked the creation of novel conceptual clusters (OCC2: t(24) = 2.8, p = 0.01; OCCP1: t(24) = 3.04, p = 0.01).

We next turned to network-level involvement in tracking Feedback-based updating. Results also did not reveal support for either PM or AT network involvement; neither PM network nor AT network estimates were significantly different from zero [PM: t(24) = -0.37, p = .71; AT: t(24) = -.341, p = .73], and estimates did not differ significantly across networks [t(24) = 0.15, p = 0.88]. Interrogation of individual ROIs also did not reveal evidence for significant involvement of any specific region (all $p > .08$; see Fig 8B).

PM and AT networks jointly support accuracy during learning

In order to determine whether computational model-based fMRI analyses were able to provide unique insights into the involvement of the PM and AT networks in the updating and use of conceptual representations, we also assessed the involvement of these networks in a univariate accuracy analysis (see Fig 9 for results from individual ROIs). One sample t-tests revealed that

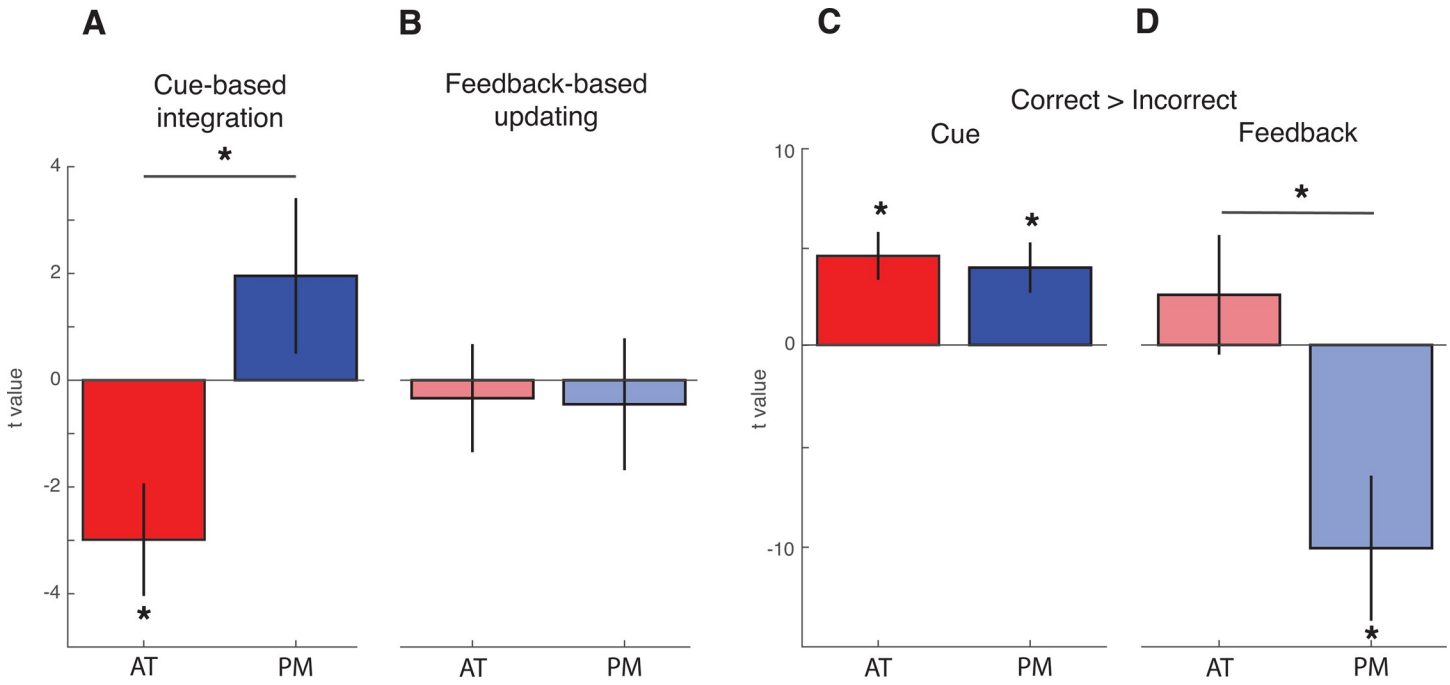

Fig 7. Model- and accuracy-based analyses in the PM and AT networks. (A) AT network is involved in integrating cue pairs within an existing cluster. Values above zero denote greater probability of assigning cue pairs to a novel cluster. Values below zero denote greater probability of capitalizing on shared features to assign cue pairs to an existing cluster. (B) Parametric activation reflecting feedback-based updating, or incremental changes to the conceptual cluster space following feedback. Positive values reflect more updating. Values below zero denote less updating. (C) Accuracy-based univariate analyses reveal that both networks demonstrate greater activation for cue pairs associated with subsequent correct relative to incorrect predictions. (D) Outcome-related univariate activation in the PM network is significantly greater for incorrect relative to correct predictions. Error bars denote standard error of the mean. * $p < .05$.

https://doi.org/10.1371/journal.pone.0207357.g007

parameter estimates were reliably different from zero in the AT network during the Cue period only [$t(24) = 3.94$, $p < .001$], whereas PM network estimates were significantly different from zero during both the Cue [$t(24) = 3.24$, $p < .01$] and Outcome [$t(24) = -2.85$, $p < .01$] trial periods (Fig 7, right panel). The resulting average parameter estimates were entered into a repeated measures ANOVA with factors for Network (PM, AT) and Trial period (Cue, Outcome). Results revealed significant main effects of Trial period ($F_{1,24} = 5.38$, $p < .05$), Network ($F_{1,24} = 27.1$, $p < .00001$) and a significant Trial period by Network interaction ($F_{1,24} = 18.9$, $p < .0001$). Follow-up paired comparisons revealed a significant difference in feedback activation for the PM and AT networks [$t(24) = 5.4$, $p < .0001$, Fig 7B] with no differences across networks during the Cue period [$t(24) = .46$, $p = .64$]. Similar results were observed when assessing Cue and Feedback activity in participants who did not display behavioral evidence of learning cue pair-outcome associations (see S2 Fig, right panel). These findings indicate that although the PM and AT networks differentially contributed to feedback learning, both displayed significant Cue period activity during trials that were associated with correct outcome decisions. These results are in contrast to the model-based analysis, which show differential PM and AT activity during the cue period.

When probing activation in individual PM and AT network ROIs, results revealed that nearly all AT network regions displayed greater Cue period activity during correct trials. Similarly, activation in half of PM network regions was also significantly greater during the Cue period of trials that were associated with correct outcome predictions (see Fig 9A and Table 1). ROI activity during the Outcome period revealed that all regions in the orbitofrontal cortex (OFC1; OFC2; OFC3; OFC4) and one fusiform ROI (FUS1) displayed greater outcome activity

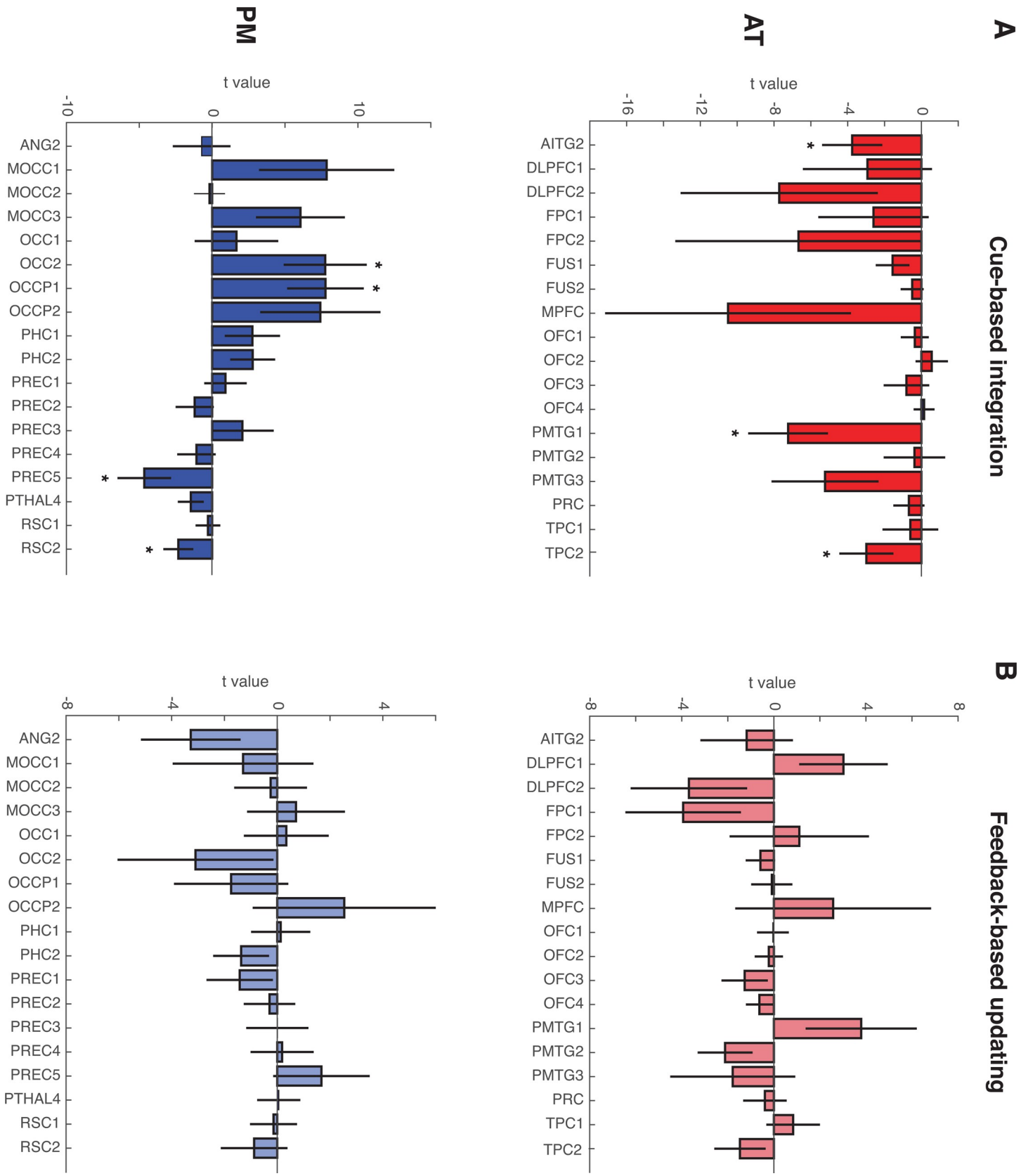
A
Cue-based integration
AT
t value
-16
-12
-8
-4
0
AITG2
DLPFC1
DLPFC2
FPC1
FPC2
FUS1
FUS2
MPFC
OFC1
OFC2
OFC3
OFC4
PMTG1
PMTG2
PMTG3
PRC
TPC1
TPC2
PM
t value
-10
0
10
ANG2
MOCC1
MOCC2
MOCC3
OCC1
OCC2
OCCP1
OCCP2
PHC1
PHC2
PREC1
PREC2
PREC3
PREC4
PREC5
PTHAL4
RSC1
RSC2
B
Feedback-based updating
t value
-8
-4
0
4
8
AITG2
DLPFC1
DLPFC2
FPC1
FPC2
FUS1
FUS2
MPFC
OFC1
OFC2
OFC3
OFC4
PMTG1
PMTG2
PMTG3
PRC
TPC1
TPC2
t value
-8
-4
0
4
ANG2
MOCC1
MOCC2
MOCC3
OCC1
OCC2
OCCP1
OCCP2
PHC1
PHC2
PREC1
PREC2
PREC3
PREC4
PREC5
PTHAL4
RSC1
RSC2

Fig 8. Model-based analyses in individual PM and AT network ROIs. (A) Cue-based integration: Negative values denote greater probability of capitalizing on shared features to assign cue pairs to an existing cluster, whereas positive values denote greater probability of assigning cue pairs to a novel cluster. Nearly all AT network ROIs demonstrate evidence for cue-based integration, with significant evidence for the involvement of posterior middle temporal gyrus, anterior inferior temporal gyri and temporopolar cortex. In the PM network, precuneus and retrosplenial cortex significantly track cue-based integration, whereas occipital regions are involved in assigning cue pairs to a novel conceptual cluster. (B) Feedback-based updating: Positive values denote larger changes to the conceptual cluster space following feedback, whereas negative values denote smaller changes. No individual regions in either network track the amount of Feedback-based updating. Error bars denote standard error of the mean. * $p < .05$.

https://doi.org/10.1371/journal.pone.0207357.g008

during correct trials, whereas PM network ROIs tended to display greater outcome activity during incorrect trials (see Fig 9B and Table 2).

Discussion

Although recent neuroimaging investigations have focused on elucidating brain regions involved in concepts formed on the basis of simple features, concepts can also reflect higher-order relationships, including shared features across entities in the environment. Here, we used computational modeling-based fMRI to assess how these types of conceptual representations are constructed and used during learning. Behavioral and model results revealed that participants who showed a tendency to link information in memory, as evidenced by the fitted coupling probability value, also had faster learning rates, suggesting that use of the conceptual structure of the task facilitated learning. Analyses of fMRI data revealed that activity in the AT network tracked the integration of cue pair information into existing conceptual clusters ("Cue-based integration"), consistent with proposals that this network encodes information about the meaning or significance of objects [13].

The present study stressed learning to integrate cues that, in isolation, were not diagnostic, in order to predict future outcomes. Additionally, although one could learn the simple associations between cue pairs and outcomes, performance could be optimized by learning concepts reflecting related events. According to cluster-based models of categorization, such as the RMC [1], categories are indirectly represented by grouping past experiences into conceptual clusters that include information about items and the categories that they had been associated with. We were especially interested in understanding how the AT and PM networks might support this process given evidence indicating that regions in the AT network represent the conceptual features of objects [20,52–55] and work that has found representations of contextual information in the PM network [25,27,32].

Results derived from the model-based fMRI analysis provide novel evidence that the AT network is involved in the integration of cue pair information into concepts that reflect shared features ("Cue-based integration"). These results complement existing fMRI evidence that have largely taken a region-specific approach as opposed to an investigation of network-wide effects. For example, a number of investigations have found evidence that the PRc is sensitive to conceptual processing [56–59] and complex conjunctions of stimulus features [60–65]. Extending these results, PRc has also been implicated in representing the significance or meaning of stimuli [17,20,21,52,66]. Consistent with a role for the AT network in integrating cue information into existing conceptual representations, prior work has also found that the OFC is critically involved in integrating prior experience with current evidence to support decisions [18,23,67,68]. Research assessing OFC involvement in learning has also found evidence that this area represents task-relevant information that cannot be directly observed [69–75], similar to the higher-order conceptual structure of the current task. Convergent results from neuropsychology have also found impairments in semantic memory and multimodal semantic processing in patients with damage to the anterior temporal lobes following semantic dementia, herpes simplex encephalitis, or temporal lobe resection [76–80], consistent with the idea that regions in this network represent conceptual and meaning-based information.

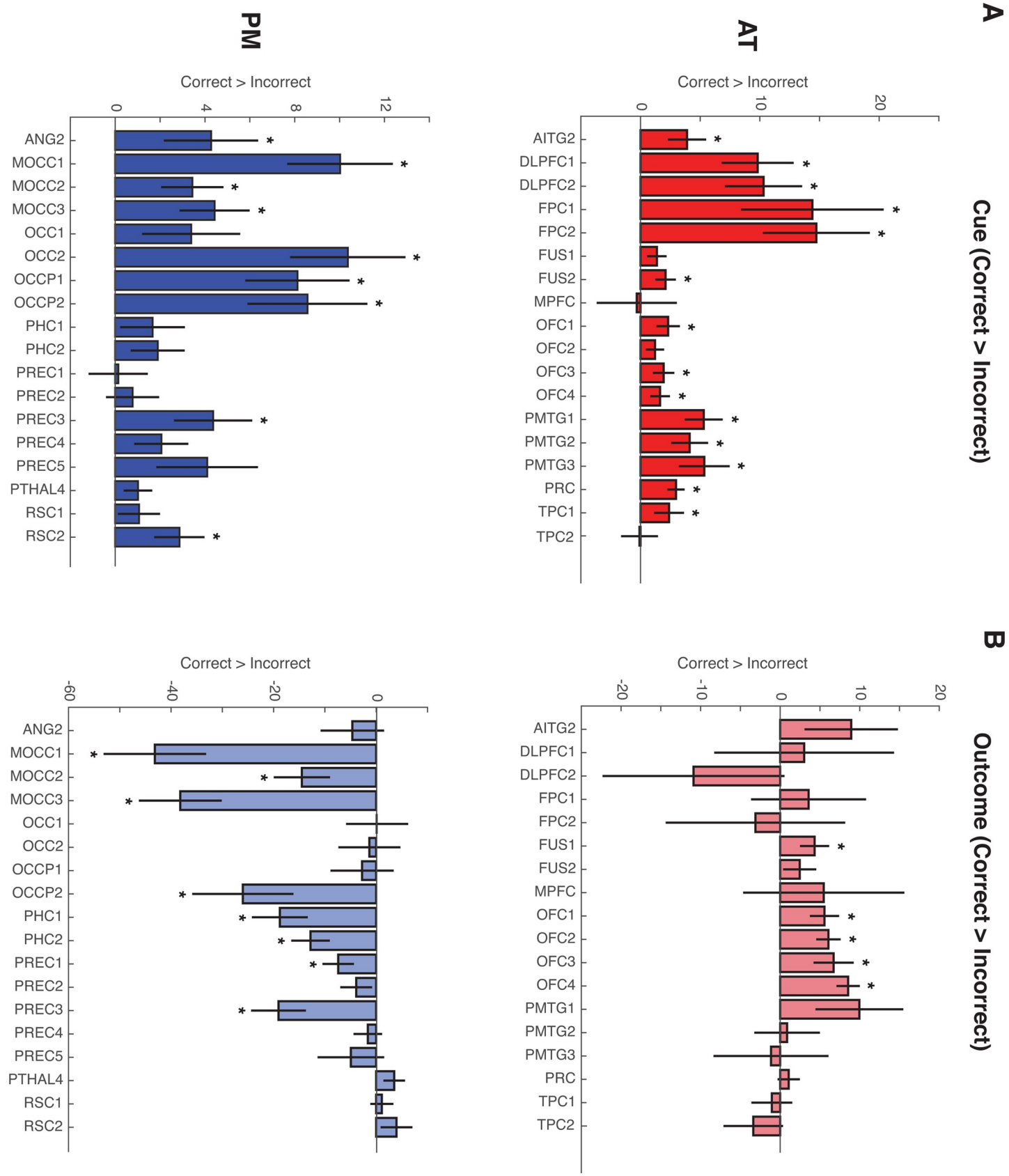
A
Cue (Correct > Incorrect)
PM
Correct > Incorrect
0
4
8
12
ANG2
MOCC1
MOCC2
MOCC3
OCC1
OCC2
OCCP1
OCCP2
PHC1
PHC2
PREC1
PREC2
PREC3
PREC4
PREC5
PTHAL4
RSC1
RSC2
AT
Correct > Incorrect
0
10
20
AITG2
DLPFC1
DLPFC2
FPC1
FPC2
FUS1
FUS2
MPFC
OFC1
OFC2
OFC3
OFC4
PMTG1
PMTG2
PMTG3
PRC
TPC1
TPC2
B
Outcome (Correct > Incorrect)
Correct > Incorrect
-60
-40
-20
0
ANG2
MOCC1
MOCC2
MOCC3
OCC1
OCC2
OCCP1
OCCP2
PHC1
PHC2
PREC1
PREC2
PREC3
PREC4
PREC5
PTHAL4
RSC1
RSC2
Correct > Incorrect
-20
-10
0
10
20
AITG2
DLPFC1
DLPFC2
FPC1
FPC2
FUS1
FUS2
MPFC
OFC1
OFC2
OFC3
OFC4
PMTG1
PMTG2
PMTG3
PRC
TPC1
TPC2

Fig 9. Accuracy-based analyses in individual PM and AT network ROIs. (A) Cue-period activity associated with Correct > Incorrect outcome judgments. The majority of PM and AT network regions display greater cue-period activation during trials that were answered correctly. (B) Outcome-related univariate activity associated with Correct > Incorrect outcome judgments. AT network ROIs, including orbitofrontal cortex and fusiform gyrus display significantly greater outcome-related activity for correctly answered trials, whereas PM network ROIs, displayed greater outcome activity during incorrect trials. Error bars denote standard error of the mean. * $p < .05$.

https://doi.org/10.1371/journal.pone.0207357.g009

Analyses of individual AT network ROIs revealed that the anterior inferior temporal gyri (AITG2), posterior middle temporal gyrus (PMTG1) and temporopolar cortex (TPC2) played a significant role in Cue-based integration. The role of these areas in learning about relevant stimulus features [81], representing a "thematic hub" of knowledge about similar associations [82], and retrieval of conceptual knowledge [83] may have made these regions particularly sensitive to learning about the shared feature structure present in the current task.

Interestingly, we did not find evidence for PM network-level involvement in indexing Cue-based integration, despite the importance of local context. One possible explanation for the lack of a broad PM network effect is the type of stimuli used in the task; regions in the PM network have typically been associated with learning and memory of contextual information that is principally spatial or location-based [32,84–90], whereas the AT network is particularly sensitive to object stimuli, such as those used in the current experiment [64,65]. It is important to note, however, that an analysis of individual PM network ROIs revealed that precuneus (PREC5) and retrosplenial cortex (RSC2) were significantly involved in tracking Cue-based integration, consistent with a role for these areas in retrieval based on internal sources of information, such as each participant's understanding of the conceptual representational space in the current task [91,92]. These results suggest that although ROIs within each network displayed more similar activity profiles than ROIs between networks (see Fig 6), individual regions may support processes that are distinct from the rest of the network. Future work will be needed to understand the conditions under which individual ROIs are engaged in similar or different processes as the rest of their affiliated network.

We additionally investigated PM involvement in tracking trial-by-trial updates to the conceptual cluster space ("Feedback-based updating") given recent proposals that this network represents the full set of relationships that are relevant in the environment [13]. Results did not

Table 1. Accuracy-based analysis—Cue period activity in individual PM and AT ROIs. Cue-period activity associated with Correct > Incorrect outcome judgments.

AT Network		PM Network	
AITG2	T(24) = 2.578, p = 0.0484	*ANG2*	T(24) = 2.08, p = 0.0483
DLPFC1	T(24) = 3.357, p = 0.0026	*MOCC1*	T(24) = 4.349, p < .0001
DLPFC2	T(24) = 3.282, p = 0.0032	*MOCC2*	T(24) = 2.563, p = 0.017
FPC1	T(24) = 2.448, p = 0.0221	*MOCC3*	T(24) = 2.925, p = 0.007
FPC2	T(24) = 3.352, p = 0.0026	*OCC2*	T(24) = 4.109, p < 0.001
FUS2	T(24) = 2.718, p = 0.0120	*OCCP1*	T(24) = 3.568, p = 0+.002
OFC1	T(24) = 2.595, p = 0.0159	*OCCP2*	T(24) = 3.264, p = 0.003
OFC3	T(24) = 3.404, p = 0.0243	*PREC3*	T(24) = 2.572, p = 0.017
OFC4	T(24) = 2.239, p = 0.0347	*RSC2*	T(24) = 2.661, p = 0.014
PMTG1	T(24) = 3.531, p = 0.0017		
PMTG2	T(24) = 2.823, p = 0.0094		
PMTG3	T(24) = 2.615, p = 0.0152		
PRC	T(24) = 4.709, p < 0.0001		
TPC1	T(24) = 2.064, p = 0.0499		

https://doi.org/10.1371/journal.pone.0207357.t001

Table 2. Accuracy-based analysis—Outcome period activity in individual PM and AT ROIs. Outcome-period activity associated with Correct > Incorrect outcome judgments.

AT Network		PM Network	
FUS1	T(24) = 2.549, p = 0.0176	*MOCC1*	T(24) = -4.408, p < .001
OFC1	T(24) = 3.276, p = 0.003	*MOCC2*	T(24) = -2.748, p = 0.011
OFC2	T(24) = 4.334, p < .001	*MOCC3*	T(24) = -4.852, p < .001
OFC3	T(24) = 2.808, p = 0.001	*OCCP2*	T(24) = -2.693, p = 0.013
OFC4	T(24) = 6.44, p < .0001	*PHC1*	T(24) = -3.59, p = 0.001
		PHC2	T(24) = -3.607, p = 0.001
		PREC1	T(24) = -2.589, p = 0.016
		PREC3	T(24) = -3.711, p = 0.001

https://doi.org/10.1371/journal.pone.0207357.t002

reveal evidence to suggest that PM network activity tracked Feedback-based updating, although PM network activation was significantly higher on incorrect trials relative to correct trials. One interpretation of these results is that the learning problem in the current task did not encourage large-scale reorganizations of the conceptual cluster space after trial-by-trial feedback [42,93]. This interpretation is consistent with individual participant behavioral learning curves and model fits, which largely depict a gradual increase in performance across the six learning runs (Fig 4). Future work will be required to assess whether and how the PM network is involved in representing or updating the full set of relationships active in the current environment.

Finally, it is interesting to consider how the current investigation complements and extends previous work. In particular, recent model-based fMRI investigations have evaluated neural evidence for different forms of category learning [94], assessed the brain areas involved in the reorganization of conceptual knowledge following changes in attention and goals [41], and identified brain regions involved in category learning with stimuli that are consistent and inconsistent with category rules [5,6]. Together these investigations have largely found evidence for hippocampal and striatal involvement, and recent theoretical work has suggested that the hippocampus may play a key role in concept formation and organization [95]. These investigations, however, have largely defined conceptual representations on the basis of simple perceptual features or associations, leaving open the question of how concepts defined on shared feature relationships are developed and used to guide learning. The current investigation suggests that these types of higher-order concepts are preferentially represented by the AT network, consistent with this network's role in representing the meaning of objects in the environment and information about complex feature conjunctions.

Supporting information

S1 Fig. Activation profile similarity analysis for poor learners only. Participants who did not display learning performance that was significantly greater than chance on the final two learning runs were included (N = 6). An activation profile similarity analysis revealed significantly higher similarity between ROIs within vs. between networks even within poor learners [t(5) = 3.67, p = .01]. Additionally, a comparison of activation profile similarity and an idealized model matrix indicated that the correlation between activation profile similarity and the model matrix was statistically significant [Kendall's tau-b = .78, p < .0001]. Purple-shaded box denotes standard deviation. Red shaded box denotes 95% confidence interval. Individual participant activation profile similarity values plotted in black. * = p < .05.
(EPS)

S2 Fig. Model- and accuracy-based analyses for poor learners only. (A) Model-based analyses: We did not observe evidence that either network was significantly involved in tracking Cue-based integration or Feedback-based updating (A repeated-measures ANOVA with factors for Network (PM, AT) and Trial period (Cue, Outcome) did not reveal evidence for any main effects or interactions (all F's < 4.6); One sample t-test: AT Cue-based integration—$t(5) = -1.68$, $p = 0.15$; PM Cue-based integration—$t(5) = 0.98$, $p = .37$; AT–Feedback-based updating—$t(5) = -.99$, $p = .36$; PM–Feedback-based updating $t(5) = -.41$; $p = .7$). (B) Accuracy-based analyses: A repeated-measures ANOVA with factors for Network (PM, AT) and Trial period (Cue, Outcome) revealed only a main effect of Network [$F(1,5) = 8.2$, $p = 0.035$; other F's < 2.18]. One-sample t-tests indicated that both the PM and AT networks were significantly active during the Cue period of correct trials [PM: $t(5) = 3.12$, $p = 0.026$; AT: $t(5) = 4.07$, $p = 0.009$]. Error bars denote standard error of the mean. * $p < .05$, one-sample t-test.
(EPS)

Acknowledgments

The authors would like to thank Maureen Ritchey for helpful discussion.

Author Contributions

Conceptualization: Marika C. Inhoff, Laura A. Libby, Charan Ranganath.

Formal analysis: Marika C. Inhoff, Takao Noguchi.

Investigation: Marika C. Inhoff, Laura A. Libby.

Resources: Bradley C. Love, Charan Ranganath.

Supervision: Bradley C. Love, Charan Ranganath.

Writing – original draft: Marika C. Inhoff, Takao Noguchi.

Writing – review & editing: Marika C. Inhoff, Laura A. Libby, Bradley C. Love, Charan Ranganath.

References

1. Anderson JR. The adaptive nature of human categorization. Psychol Rev. 1991; 98: 409.
2. Murphy G. The big book of concepts. MIT press; 2004.
3. Shea N, Krug K, Tobler PN. Conceptual representations in goal-directed decision making. Cogn Affect Behav Neurosci. 2008; 8: 418–428. https://doi.org/10.3758/CABN.8.4.418 PMID: 19033239
4. Clarke A, Pell PJ, Ranganath C, Tyler LK. Learning Warps Object Representations in the Ventral Temporal Cortex. J Cogn Neurosci. 2016; 1–14. https://doi.org/10.1162/jocn_a_00951 PMID: 26967942
5. Davis T, Love BC, Preston AR. Learning the Exception to the Rule: Model-Based fMRI Reveals Specialized Representations for Surprising Category Members. Cereb Cortex. 2012; 22: 260–273. https://doi.org/10.1093/cercor/bhr036 PMID: 21666132
6. Davis T, Love BC, Preston AR. Striatal and hippocampal entropy and recognition signals in category learning: Simultaneous processes revealed by model-based fMRI. J Exp Psychol Learn Mem Cogn. 2012b; 38: 821–839. https://doi.org/10.1037/a0027865 PMID: 22746951
7. Folstein JR, Palmeri TJ, Gauthier I. Category Learning Increases Discriminability of Relevant Object Dimensions in Visual Cortex. Cereb Cortex. 2012; 23: 814–823. https://doi.org/10.1093/cercor/bhs067 PMID: 22490547
8. Goldstone RL. Influences of categorization on perceptual discrimination. J Exp Psychol Gen. 1994; 123: 178. PMID: 8014612
9. Jiang X, Bradley E, Rini RA, Zeffiro T, VanMeter J, Riesenhuber M. Categorization Training Results in Shape- and Category-Selective Human Neural Plasticity. Neuron. 2007; 53: 891–903. https://doi.org/10.1016/j.neuron.2007.02.015 PMID: 17359923

10. Kumaran D, Summerfield JJ, Hassabis D, Maguire EA. Tracking the Emergence of Conceptual Knowledge during Human Decision Making. Neuron. 2009; 63: 889–901. https://doi.org/10.1016/j.neuron.2009.07.030 PMID: 19778516
11. Zeithamova D, Maddox WT, Schnyer DM. Dissociable Prototype Learning Systems: Evidence from Brain Imaging and Behavior. J Neurosci. 2008; 28: 13194–13201. https://doi.org/10.1523/JNEUROSCI.2915-08.2008 PMID: 19052210
12. Inhoff MC, Ranganath C. Dynamic cortico-hippocampal networks underlying memory and cognition: the PMAT framework. The Hippocampus from Cells to Systems: Structure, Connectivity, and Functional Contributions to Memory and Flexible Cognition. Springer; 2017.
13. Ranganath C, Ritchey M. Two cortical systems for memory-guided behaviour. Nat Rev Neurosci. 2012; 13: 713–726. https://doi.org/10.1038/nrn3338 PMID: 22992647
14. Ritchey M, Libby LA, Ranganath C. Cortico-hippocampal systems involved in memory and cognition: the PMAT framework. Progress in Brain Research. Elsevier; 2015. pp. 45–64. Available: http://linkinghub.elsevier.com/retrieve/pii/S0079612315000588
15. Bussey TJ, Saksida LM, Murray EA. The perceptual-mnemonic/feature conjunction model of perirhinal cortex function. Q J Exp Psychol Sect B. 2005; 58: 269–282.
16. Chan SCY, Niv Y, Norman KA. A Probability Distribution over Latent Causes, in the Orbitofrontal Cortex. J Neurosci. 2016; 36: 7817–7828. https://doi.org/10.1523/JNEUROSCI.0659-16.2016 PMID: 27466328
17. Clarke A, Tyler LK. Object-Specific Semantic Coding in Human Perirhinal Cortex. J Neurosci. 2014; 34: 4766–4775. https://doi.org/10.1523/JNEUROSCI.2828-13.2014 PMID: 24695697
18. Farovik A, Place RJ, McKenzie S, Porter B, Munro CE, Eichenbaum H. Orbitofrontal Cortex Encodes Memories within Value-Based Schemas and Represents Contexts That Guide Memory Retrieval. J Neurosci. 2015; 35: 8333–8344. https://doi.org/10.1523/JNEUROSCI.0134-15.2015 PMID: 26019346
19. Gallagher M, McMahan RW, Schoenbaum G. Orbitofrontal cortex and representation of incentive value in associative learning. J Neurosci. 1999; 19: 6610–6614. PMID: 10414988
20. Inhoff MC, Ranganath C. Significance of objects in the perirhinal cortex. Trends Cogn Sci. 2015; 19: 302–303. https://doi.org/10.1016/j.tics.2015.04.008 PMID: 25979850
21. Kivisaari SL, Tyler LK, Monsch AU, Taylor KI. Medial perirhinal cortex disambiguates confusable objects. Brain. 2012; 135: 3757–3769. https://doi.org/10.1093/brain/aws277 PMID: 23250887
22. Martin CB, Douglas D, Newsome RN, Man LLY, Barense MD. Integrative and distinctive coding of visual and conceptual features in the ventral visual stream. eLife. 2018; 7. https://doi.org/10.7554/eLife.31873 PMID: 29393853
23. Nogueira R, Abolafia JM, Drugowitsch J, Balaguer-Ballester E, Sanchez-Vives MV, Moreno-Bote R. Lateral orbitofrontal cortex anticipates choices and integrates prior with current information. Nat Commun. 2017; 8: 14823. https://doi.org/10.1038/ncomms14823 PMID: 28337990
24. Aminoff EM, Kveraga K, Bar M. The role of the parahippocampal cortex in cognition. Trends Cogn Sci. 2013; 17: 379–390. https://doi.org/10.1016/j.tics.2013.06.009 PMID: 23850264
25. Bar M, Aminoff E, Schacter DL. Scenes Unseen: The Parahippocampal Cortex Intrinsically Subserves Contextual Associations, Not Scenes or Places Per Se. J Neurosci. 2008; 28: 8539–8544. https://doi.org/10.1523/JNEUROSCI.0987-08.2008 PMID: 18716212
26. Davachi L. Item, context and relational episodic encoding in humans. Curr Opin Neurobiol. 2006; 16: 693–700. https://doi.org/10.1016/j.conb.2006.10.012 PMID: 17097284
27. Diana RA, Yonelinas AP, Ranganath C. Imaging recollection and familiarity in the medial temporal lobe: a three-component model. Trends Cogn Sci. 2007; 11: 379–386. https://doi.org/10.1016/j.tics.2007.08.001 PMID: 17707683
28. Diana RA, Yonelinas AP, Ranganath C. Medial temporal lobe activity during source retrieval reflects information type, not memory strength. J Cogn Neurosci. 2009; 22: 1808–1818.
29. Diana RA, Yonelinas AP, Ranganath C. Adaptation to cognitive context and item information in the medial temporal lobes. Neuropsychologia. 2012; 50: 3062–3069. https://doi.org/10.1016/j.neuropsychologia.2012.07.035 PMID: 22846335
30. Eacott MJ, Gaffan EA. The roles of perirhinal cortex, postrhinal cortex, and the fornix in memory for objects, contexts, and events in the rat. Q J Exp Psychol Sect B. 2005; 58: 202–217. https://doi.org/10.1080/02724990444000203 PMID: 16194965
31. Eichenbaum H, Yonelinas AR, Ranganath C. The medial temporal lobe and recognition memory. Annu Rev Neurosci. 2007; 30: 123. https://doi.org/10.1146/annurev.neuro.30.051606.094328 PMID: 17417939

32. Staresina BP, Duncan KD, Davachi L. Perirhinal and Parahippocampal Cortices Differentially Contribute to Later Recollection of Object- and Scene-Related Event Details. J Neurosci. 2011; 31: 8739–8747. https://doi.org/10.1523/JNEUROSCI.4978-10.2011 PMID: 21677158

33. Epstein RA. Parahippocampal and retrosplenial contributions to human spatial navigation. Trends Cogn Sci. 2008; 12: 388–396. https://doi.org/10.1016/j.tics.2008.07.004 PMID: 18760955

34. Todd TP, Meyer HC, Bucci DJ. Contribution of the retrosplenial cortex to temporal discrimination learning: Retrosplenial and Temporal Context. Hippocampus. 2015; 25: 137–141. https://doi.org/10.1002/hipo.22385 PMID: 25348829

35. Vann SD, Aggleton JP, Maguire EA. What does the retrosplenial cortex do? Nat Rev Neurosci. 2009; 10: 792–802. https://doi.org/10.1038/nrn2733 PMID: 19812579

36. Vann SD, Aggleton JP. Extensive cytotoxic lesions of the rat retrosplenial cortex revel consistent deficits on tasks that tax allocentric spatial memory. Behav Neurosci. 2002; 116: 85–94. https://doi.org/10.1037//0735-7044.116.1.85 PMID: 11895186

37. Cabeza R, Ciaramelli E, Olson IR, Moscovitch M. The parietal cortex and episodic memory: an attentional account. Nat Rev Neurosci. 2008; 9: 613–625. https://doi.org/10.1038/nrn2459 PMID: 18641668

38. Vilberg KL, Rugg MD. Memory retrieval and the parietal cortex: A review of evidence from a dual-process perspective. Neuropsychologia. 2008; 46: 1787–1799. https://doi.org/10.1016/j.neuropsychologia.2008.01.004 PMID: 18343462

39. Konkle T, Brady TF, Alvarez GA, Oliva A. Conceptual distinctiveness supports detailed visual long-term memory for real-world objects. J Exp Psychol Gen. 2010; 139: 558–578. https://doi.org/10.1037/a0019165 PMID: 20677899

40. Love BC, Gureckis TM. Models in search of a brain. Cogn Affect Behav Neurosci. 2007; 7: 90–108. PMID: 17672381

41. Mack ML, Love BC, Preston AR. Dynamic updating of hippocampal object representations reflects new conceptual knowledge. Proc Natl Acad Sci. 2016; 113: 13203–13208. https://doi.org/10.1073/pnas.1614048113 PMID: 27803320

42. Sanborn AN, Griffiths TL, Navarro DJ. Rational approximations to rational models: Alternative algorithms for category learning. Psychol Rev. 2010; 117: 1144–1167. https://doi.org/10.1037/a0020511 PMID: 21038975

43. Jenkinson M, Bannister P, Brady M, Smith S. Improved Optimization for the Robust and Accurate Linear Registration and Motion Correction of Brain Images. NeuroImage. 2002; 17: 825–841. https://doi.org/10.1006/nimg.2002.1132 PMID: 12377157

44. Smith SM. Fast robust automated brain extraction. Hum Brain Mapp. 2002; 17: 143–155. https://doi.org/10.1002/hbm.10062 PMID: 12391568

45. Jenkinson M, Smith S. A global optimisation method for robust affine registration of brain images. Med Image Anal. 2001; 5: 143–156. PMID: 11516708

46. Woolrich MW, Ripley BD, Brady M, Smith SM. Temporal Autocorrelation in Univariate Linear Modeling of FMRI Data. NeuroImage. 2001; 14: 1370–1386. https://doi.org/10.1006/nimg.2001.0931 PMID: 11707093

47. Libby LA, Ekstrom AD, Ragland JD, Ranganath C. Differential Connectivity of Perirhinal and Parahippocampal Cortices within Human Hippocampal Subregions Revealed by High-Resolution Functional Imaging. J Neurosci. 2012; 32: 6550–6560. https://doi.org/10.1523/JNEUROSCI.3711-11.2012 PMID: 22573677

48. Ritchey M, Yonelinas AP, Ranganath C. Functional Connectivity Relationships Predict Similarities in Task Activation and Pattern Information during Associative Memory Encoding. J Cogn Neurosci. 2014; 26: 1085–1099. https://doi.org/10.1162/jocn_a_00533 PMID: 24283495

49. Beckmann CF, Jenkinson M, Smith SM. General multilevel linear modeling for group analysis in FMRI. NeuroImage. 2003; 20: 1052–1063. https://doi.org/10.1016/S1053-8119(03)00435-X PMID: 14568475

50. Woolrich MW, Behrens TEJ, Beckmann CF, Jenkinson M, Smith SM. Multilevel linear modelling for FMRI group analysis using Bayesian inference. NeuroImage. 2004; 21: 1732–1747. https://doi.org/10.1016/j.neuroimage.2003.12.023 PMID: 15050594

51. Woolrich M. Robust group analysis using outlier inference. NeuroImage. 2008; 41: 286–301. https://doi.org/10.1016/j.neuroimage.2008.02.042 PMID: 18407525

52. Clarke A, Tyler LK. Understanding What We See: How We Derive Meaning From Vision. Trends Cogn Sci. 2015; 19: 677–687. https://doi.org/10.1016/j.tics.2015.08.008 PMID: 26440124

53. Murray E., Wise SP, Graham KS. The evolution of memory systems: Ancestors, anatomy and adaptation. Oxford University Press, Oxford; 2017.

54. Olson IR, Plotzker A, Ezzyat Y. The Enigmatic temporal pole: a review of findings on social and emotional processing. Brain. 2007; 130: 1718–1731. https://doi.org/10.1093/brain/awm052 PMID: 17392317

55. Von Der Heide RJ, Skipper LM, Klobusicky E, Olson IR. Dissecting the uncinate fasciculus: disorders, controversies and a hypothesis. Brain. 2013; 136: 1692–1707. https://doi.org/10.1093/brain/awt094 PMID: 23649697

56. Heusser AC, Awipi T, Davachi L. The ups and downs of repetition: Modulation of the perirhinal cortex by conceptual repetition predicts priming and long-term memory. Neuropsychologia. 2013; 51: 2333–2343. https://doi.org/10.1016/j.neuropsychologia.2013.04.018 PMID: 23651708

57. O'Kane G, Insler RZ, Wagner AD. Conceptual and perceptual novelty effects in human medial temporal cortex. Hippocampus. 2005; 15: 326–332. https://doi.org/10.1002/hipo.20053 PMID: 15490462

58. Wang W-C, Lazzara MM, Ranganath C, Knight RT, Yonelinas AP. The Medial Temporal Lobe Supports Conceptual Implicit Memory. Neuron. 2010; 68: 835–842. https://doi.org/10.1016/j.neuron.2010.11.009 PMID: 21144998

59. Wang W-C, Ranganath C, Yonelinas AP. Activity reductions in perirhinal cortex predict conceptual priming and familiarity-based recognition. Neuropsychologia. 2014; 52: 19–26. https://doi.org/10.1016/j.neuropsychologia.2013.10.006 PMID: 24157537

60. Barense, Gaffan D, Graham KS. The human medial temporal lobe processes online representations of complex objects. Neuropsychologia. 2007; 45: 2963–2974. https://doi.org/10.1016/j.neuropsychologia.2007.05.023 PMID: 17658561

61. Barense, Rogers TT, Bussey TJ, Saksida LM, Graham KS. Influence of Conceptual Knowledge on Visual Object Discrimination: Insights from Semantic Dementia and MTL Amnesia. Cereb Cortex. 2010; 20: 2568–2582. https://doi.org/10.1093/cercor/bhq004 PMID: 20150429

62. Buckley MJ, Booth MC., Rolls ET, Gaffan D. Selective perceptual impairments after perirhinal cortex ablation. J Neurosci. 2001; 21: 9824–9836. PMID: 11739590

63. Mion M, Patterson K, Acosta-Cabronero J, Pengas G, Izquierdo-Garcia D, Hong YT, et al. What the left and right anterior fusiform gyri tell us about semantic memory. Brain. 2010; 133: 3256–3268. https://doi.org/10.1093/brain/awq272 PMID: 20952377

64. Moss HE, Rodd J., Stamatakis EA, Bright P, Tyler LK. Anteromedial Temporal Cortex Supports Fine-grained Differentiation among Objects. Cereb Cortex. 2004; 15: 616–627. https://doi.org/10.1093/cercor/bhh163 PMID: 15342435

65. Murray EA, Richmond BJ. Role of perirhinal cortex in object perception, memory, and associations. Curr Opin Neurobiol. 2001; 11: 188–193. PMID: 11301238

66. Eradath MK, Mogami T, Wang G, Tanaka K. Time Context of Cue-Outcome Associations Represented by Neurons in Perirhinal Cortex. J Neurosci. 2015; 35: 4350–4365. https://doi.org/10.1523/JNEUROSCI.4730-14.2015 PMID: 25762680

67. Ramus SJ, Eichenbaum H. Neural correlates of olfactory recognition memory in the rat orbitofrontal cortex. J Neurosci. 2000; 20: 8199–8208. PMID: 11050143

68. Schoenbaum G, Eichenbaum H. Information coding in the rodent prefrontal cortex. I. Single-neuron activity in orbitofrontal cortex compared with that in pyriform cortex. J Neurophysiol. 1995; 74: 733–750. https://doi.org/10.1152/jn.1995.74.2.733 PMID: 7472378

69. Bradfield LA, Dezfouli A, van Holstein M, Chieng B, Balleine BW. Medial Orbitofrontal Cortex Mediates Outcome Retrieval in Partially Observable Task Situations. Neuron. 2015; 88: 1268–1280. https://doi.org/10.1016/j.neuron.2015.10.044 PMID: 26627312

70. Courville AC, Daw ND, Touretzky DS. Similarity and discrimination in classical conditioning: A latent variable account. Advances in neural information processing systems. 2005. pp. 313–320.

71. Gershman SJ, Blei DM, Niv Y. Context, learning, and extinction. Psychol Rev. 2010; 117: 197–209. https://doi.org/10.1037/a0017808 PMID: 20063968

72. Gershman SJ, Niv Y. Learning latent structure: carving nature at its joints. Curr Opin Neurobiol. 2010; 20: 251–256. https://doi.org/10.1016/j.conb.2010.02.008 PMID: 20227271

73. Schuck NW, Cai MB, Wilson RC, Niv Y. Human Orbitofrontal Cortex Represents a Cognitive Map of State Space. Neuron. 2016; 91: 1402–1412. https://doi.org/10.1016/j.neuron.2016.08.019 PMID: 27657452

74. Wikenheiser AM, Schoenbaum G. Over the river, through the woods: cognitive maps in the hippocampus and orbitofrontal cortex. Nat Rev Neurosci. 2016; 17: 513–523. https://doi.org/10.1038/nrn.2016.56 PMID: 27256552

75. Wilson RC, Takahashi YK, Schoenbaum G, Niv Y. Orbitofrontal Cortex as a Cognitive Map of Task Space. Neuron. 2014; 81: 267–279. https://doi.org/10.1016/j.neuron.2013.11.005 PMID: 24462094

76. Nestor PJ, Fryer TD, Hodges JR. Declarative memory impairments in Alzheimer's disease and semantic dementia. NeuroImage. 2006; 30: 1010–1020. https://doi.org/10.1016/j.neuroimage.2005.10.008 PMID: 16300967

77. Noppeney U, Patterson K, Tyler LK, Moss H, Stamatakis EA, Bright P, et al. Temporal lobe lesions and semantic impairment: a comparison of herpes simplex virus encephalitis and semantic dementia. Brain. 2006; 130: 1138–1147. https://doi.org/10.1093/brain/awl344 PMID: 17251241

78. Binney RJ, Embleton KV, Jefferies E, Parker GJM, Lambon Ralph MA. The Ventral and Inferolateral Aspects of the Anterior Temporal Lobe Are Crucial in Semantic Memory: Evidence from a Novel Direct Comparison of Distortion-Corrected fMRI, rTMS, and Semantic Dementia. Cereb Cortex. 2010; 20: 2728–2738. https://doi.org/10.1093/cercor/bhq019 PMID: 20190005

79. Sharp DJ, Scott SK, Wise RJS. Retrieving meaning after temporal lobe infarction: The role of the basal language area. Ann Neurol. 2004; 56: 836–846. https://doi.org/10.1002/ana.20294 PMID: 15514975

80. Vandenberghe R, Price C, Wise R, Josephs O, Frackowiak RSJ. Functional anatomy of a common semantic system for words and pictures. Nature. 1996; 383: 254–256. https://doi.org/10.1038/383254a0 PMID: 8805700

81. Jagadeesh B, Chelazzi L, Mishkin M, Desimone R. Learning Increases Stimulus Salience in Anterior Inferior Temporal Cortex of the Macaque. J Neurophysiol. 2001; 86: 290–303. https://doi.org/10.1152/jn.2001.86.1.290 PMID: 11431510

82. Schwartz MF, Kimberg DY, Walker GM, Brecher A, Faseyitan OK, Dell GS, et al. Neuroanatomical dissociation for taxonomic and thematic knowledge in the human brain. Proc Natl Acad Sci. 2011; 108: 8520–8524. https://doi.org/10.1073/pnas.1014935108 PMID: 21540329

83. Davey J, Cornelissen PL, Thompson HE, Sonkusare S, Hallam G, Smallwood J, et al. Automatic and Controlled Semantic Retrieval: TMS Reveals Distinct Contributions of Posterior Middle Temporal Gyrus and Angular Gyrus. J Neurosci. 2015; 35: 15230–15239. https://doi.org/10.1523/JNEUROSCI.4705-14.2015 PMID: 26586812

84. Bachevalier J, Nemanic S. Memory for spatial location and object-place associations are differently processed by the hippocampal formation, parahippocampal areas TH/TF and perirhinal cortex. Hippocampus. 2008; 18: 64–80. https://doi.org/10.1002/hipo.20369 PMID: 17924520

85. Brewer JB, Zhao Z, Desmond JE, Glover GH, Gabrieli JD. Making memories: brain activity that predicts how well visual experience will be remembered. Science. 1998; 281: 1185–1187. PMID: 9712581

86. Dilks DD, Julian JB, Kubilius J, Spelke ES, Kanwisher N. Mirror-Image Sensitivity and Invariance in Object and Scene Processing Pathways. J Neurosci. 2011; 31: 11305–11312. https://doi.org/10.1523/JNEUROSCI.1935-11.2011 PMID: 21813690

87. Epstein RA, Parker WE, Feiler AM. Where Am I Now? Distinct Roles for Parahippocampal and Retrosplenial Cortices in Place Recognition. J Neurosci. 2007; 27: 6141–6149. https://doi.org/10.1523/JNEUROSCI.0799-07.2007 PMID: 17553986

88. Morgan LK, MacEvoy SP, Aguirre GK, Epstein RA. Distances between Real-World Locations Are Represented in the Human Hippocampus. J Neurosci. 2011; 31: 1238–1245. https://doi.org/10.1523/JNEUROSCI.4667-10.2011 PMID: 21273408

89. Norman G, Eacott MJ. Dissociable Effects of Lesions to the Perirhinal Cortex and the Postrhinal Cortex on Memory for Context and Objects in Rats. Behav Neurosci. 2005; 119: 557–566. https://doi.org/10.1037/0735-7044.119.2.557 PMID: 15839802

90. Stern CE, Corkin S, González RG, Guimaraes AR, Baker JR, Jennings PJ, et al. The hippocampal formation participates in novel picture encoding: evidence from functional magnetic resonance imaging. Proc Natl Acad Sci. 1996; 93: 8660–8665. PMID: 8710927

91. Raichle ME, MacLeod AM, Snyder AZ, Powers WJ, Gusnard DA, Shulman GL. A default mode of brain function. Proc Natl Acad Sci. 2001; 98: 676–682. https://doi.org/10.1073/pnas.98.2.676 PMID: 11209064

92. Cavanna AE, Trimble MR. The precuneus: a review of its functional anatomy and behavioural correlates. Brain. 2006; 129: 564–583. https://doi.org/10.1093/brain/awl004 PMID: 16399806

93. Love BC, Medin DL, Gureckis TM. SUSTAIN: A Network Model of Category Learning. Psychol Rev. 2004; 111: 309–332. https://doi.org/10.1037/0033-295X.111.2.309 PMID: 15065912

94. Mack ML, Preston AR, Love BC. Decoding the Brain's Algorithm for Categorization from Its Neural Implementation. Curr Biol. 2013; 23: 2023–2027. https://doi.org/10.1016/j.cub.2013.08.035 PMID: 24094852

95. Mack ML, Love BC, Preston AR. Building concepts one episode at a time: The hippocampus and concept formation. Neurosci Lett. 2017; https://doi.org/10.1016/j.neulet.2017.07.061 PMID: 28801273